Supplementary Information

Synthesis of nickel(II)-containing *meso*-edited phthalocyanine derivatives

Yuta Takiya, Taiga Saito, Naoyuki Toriumi,* and Masanobu Uchiyama*

Table of Contents

1. General

Instrumentation.

^{1}H and ^{13}C NMR spectra were obtained on a Bruker AVANCE NEO 500 spectrometer. Samples were recorded in $CDCl_3$, CD_2Cl_2, pyridine-d_5, DMSO-d_6, or THF-d_8. Chemical shifts are expressed in δ (ppm) values. ^{1}H spectra were referenced to tetramethylsilane (δ = 0.00 ppm), residual $CHCl_3$ (δ = 7.26 ppm), residual $CHDCl_2$ (δ = 5.32 ppm), residual pyridine-d_4 (δ = 8.74 ppm), residual DMSO-d_5 (δ = 2.50 ppm), or residual THF-d_7 (δ = 3.50 ppm) as an internal standard. ^{13}C spectra were referenced to tetramethylsilane (δ = 0.00 ppm) or $CDCl_3$ (δ = 77.16 ppm) as an internal standard. The following abbreviations are used: s = singlet, d = doublet, t = triplet, sept = septet, m = multiplet, br = broad. ESR spectra were obtained on a JEOL JES-X320 spectrometer. IR spectra were obtained on a JASCO FT/IR 4700 spectrometer. ESI-MS spectra were measured on a Bruker compact spectrometer. Ultraviolet-visible-near-IR absorption spectra were recorded with a JASCO V-770 spectrophotometer. Emission spectra were recorded on a JASCO FP-8750 spectrofluorometer. Cyclic voltammetry measurements were carried out with a Hokuto Denko HZ-110 voltammetric analyzer. Single crystal X-ray analysis was performed with a Rigaku XtaLAB Synergy-S diffractometer with a HyPix-6000HE HPC detector. All the reactions were performed under an Ar atmosphere using a standard Schlenk technique or an Ar glovebox (MBRAUN, Labmaster Pro).

Materials.

Unless otherwise noted, materials were purchased from Merck-Sigma-Aldrich Corporation, FUJIFILM Wako Pure Chemical Corporation, Tokyo Chemical Industry Corporation, and Kanto Chemical Corporation.

Dehydrated toluene, CH_2Cl_2, and tetrahydrofuran (THF) were purchased from Kanto Chemical and purified by a solvent purification system of Glass-Contour. Flash column chromatographic separation was performed with Yamazen medium pressure liquid chromatography (MPLC) system (EPCLC-W-Prep 2XY A-Type) using a disposable Hi-flash column from Yamazen Co. Merck Kiesel gel 60 F_{254} plate (0.25 mm thickness, coated on glass 20×20 cm^2) was used for analytical thin layer chromatography (TLC).

2. Experimental Details

2-1. Synthesis of Compounds

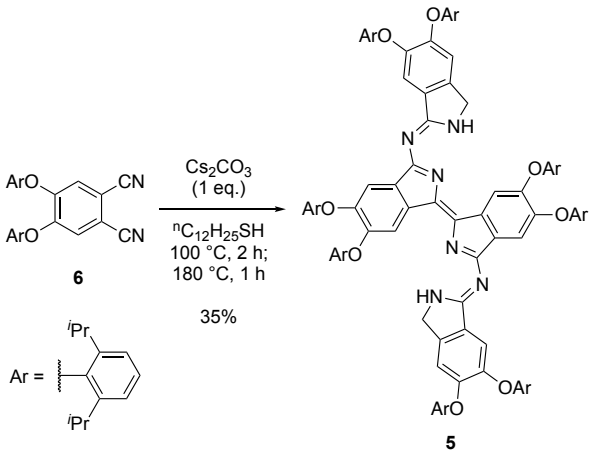

A suspension of cesium carbonate (702.0 mg, 2.155 mmol, 1.0 eq.) in dodecanethiol (4.0 mL) was stirred at 100 °C for 5 min. Then, to the suspension was added **6**[1] (1006.5 mg, 2.094 mmol, 1.0 eq.). The mixture was stirred at 100 °C for 2 h and 180 °C for 1 h. The black suspension was quenched with $NaHCO_3$ aq., extracted with $CHCl_3$ three times, washed with water, and evaporated *in vacuo*. Column chromatography on silica gel using $CHCl_3$/hexane (60:40) as an eluent gave the desired compound **5** as a red solid (348.8 mg, 35%). The spectroscopic data agreed with those in the literature.[2]

^{1}H-NMR (500 MHz, $CDCl_3$/TMS): δ 7.56 (s, 2H), 7.40–7.32 (m, 10H), 7.28 (d, 4H, J = 7.5 Hz), 7.24 (d, 4H, 7.7 Hz), 7.16 (d, 4H, 7.7 Hz), 7.06 (t, 2H, J = 7.6 Hz), 6.89 (s, 2H), 6.74 (s, 2H), 6.50 (s, 2H), 3.94 (s, 2H), 3.27–3.10 (m, 16H), 1.34–0.99 (m, 96H).

^{13}C-NMR (126 MHz, $CDCl_3$/TMS): δ 170.4, 164.0, 151.3, 149.0, 148.9, 148.8, 148.7, 148.51, 148.47, 148.4, 143.3, 142.0, 141.7, 141.6, 141.4, 136.3, 133.0, 132.3, 128.23, 126.22, 126.17, 125.8, 125.3, 124.7, 124.6, 124.5, 124.3, 109.6, 108.2, 107.3, 106.6, 50.0, 27.4, 27.28, 27.27, 27.2, 24.2, 23.8, 23.2, 22.8.

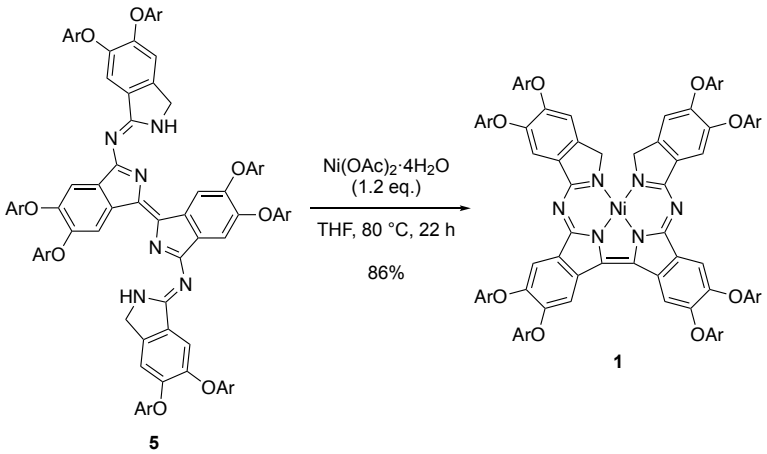

5 (100.0 mg, 52.6 μmol, 1.0 eq.) and $Ni(OAc)_2 \cdot 4H_2O$ (15.75 mg, 63.3 μmol, 1.2 eq.) were mixed in THF (5 mL) and stirred at 80 °C for 22 h. The red solution was evaporated *in vacuo*. Column chromatography on silica gel using $CHCl_3$/hexane (28:72 to 80:20) as an eluent gave the desired compound **1** as a red solid (88.8 mg, 86%).

^{1}H-NMR (500 MHz, $CDCl_3$/TMS): δ 7.38 (t, 2H, *J* = 7.7 Hz), 7.35–7.27 (m, 8H), 7.25–7.20 (m, 8H), 7.19–7.14 (m, 4H), 7.14–7.09 (m, 2H), 7.01 (s, 2H), 6.92 (s, 2H), 6.78 (s, 2H), 6.53 (s, 2H), 4.45 (s, 4H), 3.27 (sept, 4H, *J* = 6.8 Hz), 3.22–3.11 (m, 8H), 2.87 (sept, 4H, *J* = 6.8 Hz), 1.32–0.90 (m, 96H).

^{13}C-NMR (126 MHz, $CDCl_3$/TMS): δ 167.0 156.6, 150.7, 150.3, 149.3, 149.2, 148.8, 148.0, 147.7, 141.8, 141.54, 141.51, 140.5, 139.6, 135.1, 131.64, 131.60, 128.1, 126.2, 126.1, 125.9, 125.5, 124.6, 124.5, 124.4, 124.1, 110.4, 108.0, 107.5, 106.4, 63.1, 27.4, 27.2, 27.1, 26.7, 24.2, 23.8, 23.1, 22.9.

UV/vis/NIR ($CHCl_3$): λ_{max} ($\varepsilon \times 10^{-4}$) = 536 (7.95), 500 (6.99), 354 (8.93) nm.

IR (ATR): 2961, 1549, 1429, 1326, 1279, 1188, 1096, 852, 775 cm^{-1}.

HRMS (ESI): *m*/*z*: $[M+H]^+$ Calcd for $C_{128}H_{149}N_6NiO_8$ 1956.0785; Found 1956.0774.

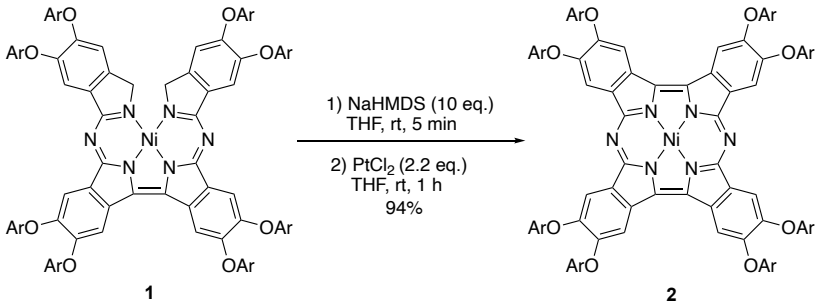

1 **2**

To a solution of **1** (20.8 mg, 10.6 μmol, 1.0 eq.) in THF (2 mL) was added NaHMDS (1.0 M in THF, 100 μL, 100 μmol, 10 eq.) at room temperature in a J-Young Schlenk flask in an Ar glovebox, and the dark brown solution was stirred at room temperature for 5 min. Then, to the solution was added a suspension of $PtCl_2$ (6.2 mg, 23 μmol, 2.2 eq) in THF (3 mL) at room temperature. The sealed flask was removed from the glovebox, and the brown solution was stirred at room temperature for 1 h. The solution was evaporated *in vacuo*. Column chromatography on silica gel using EtOAc/hexane (hexane only to 15:85) as an eluent gave the desired compound **2** as a brown solid (19.5 mg, 94%).

^{1}H-NMR (500 MHz, $CDCl_3$/TMS): δ 7.11 (t, 4H, *J* = 7.6 Hz), 7.08–7.00 (m, 20H), 5.66 (s, 4H), 5.56 (s, 4H), 3.03 (sept, 8H, *J* = 6.8 Hz), 2.67 (sept, 8H, *J* = 6.8 Hz), 1.09 (d, 48H, *J* = 6.9 Hz), 1.06–0.91 (m, 48H). **^{1}H-NMR (500 MHz, pyridine-*d*$_5$):** δ 7.47–7.44 (m, 4H), 7.27–7.25 (m, 20H), 6.17 (s, 4H), 5.91 (s, 4H), 3.38 (sept, 8H, *J* = 7.0 Hz), 2.94 (sept, 8H, *J* = 7.0 Hz), 1.28–1.04 (m, 96H).

^{13}C-NMR (126 MHz, $CDCl_3$/TMS): δ 163.0, 149.8, 149.2, 148.6, 147.4, 141.1, 140.5, 134.8, 133.3, 129.0, 126.0, 125.6, 124.4, 124.1, 111.5, 108.6, 27.2, 26.7, 24.2, 23.5, 23.0.

UV/vis/NIR ($CHCl_3$): λ_{max} ($\varepsilon \times 10^{-4}$) = 751 (0.269), 412 (5.67) nm.

IR (ATR): 2962, 1438, 1392, 1325, 1258, 1183, 1093, 896, 781, 669 cm^{-1}.

HRMS (ESI): *m*/*z*: $[M+H]^+$ Calcd for $C_{128}H_{145}N_6NiO_8$ 1952.0472; Found 1952.0465.

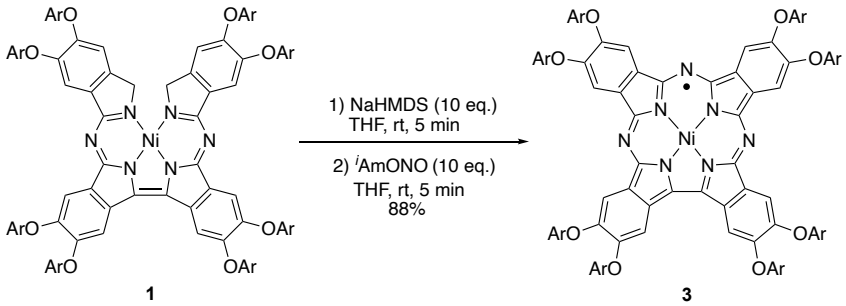

To a solution of **1** (19.6 mg, 10.0 μmol, 1.0 eq.) in THF (6 mL) was added NaHMDS (1.0 M in THF, 100 μL, 100 μmol, 10 eq.) at room temperature in a J-Young Schlenk flask in an Ar glovebox, and the dark brown solution was stirred at room temperature for 5 min. The sealed flask was removed from the glovebox, and to the solution was added isoamyl nitrite (13.5 μL, 100 μmol, 10 eq.) at room temperature. Then, the green solution was stirred at room temperature for 5 min. The solution was evaporated *in vacuo*. Column chromatography on silica gel using EtOAc/hexane (13:87) as an eluent gave the desired compound **3** as a green solid (17.4 mg, 88%).

UV/vis/NIR ($CHCl_3$): λ_{max} ($\varepsilon \times 10^{-4}$) = 1431 (0.0640), 1193 (0.0698), 770 (0.837), 679 (0.910), 397 (3.70) nm.

IR (ATR): 2961, 1438, 1327, 1271, 1189, 1095, 879, 781, 668 cm^{-1}

HRMS (ESI): *m/z*: $[M]^+$ Calcd for $C_{128}H_{144}N_7NiO_8$ 1965.0424; Found 1965.0418.

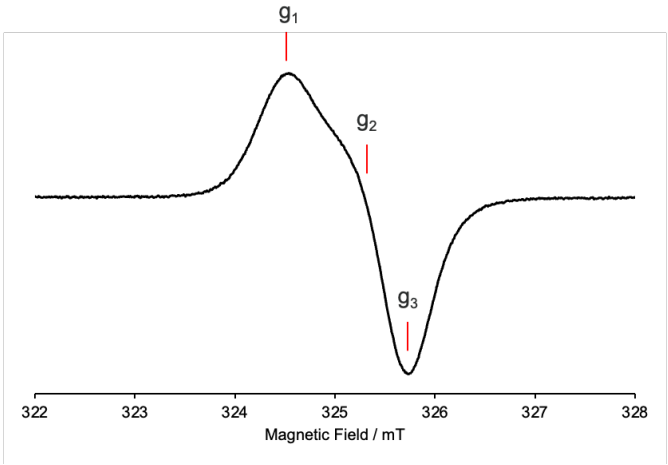

Supplementary Fig. 1. ESR spectrum of **3** in toluene at –150 °C (9125 MHz) (g_1 =2.0091, g_2 =2.0043, g_3 =2.0015).

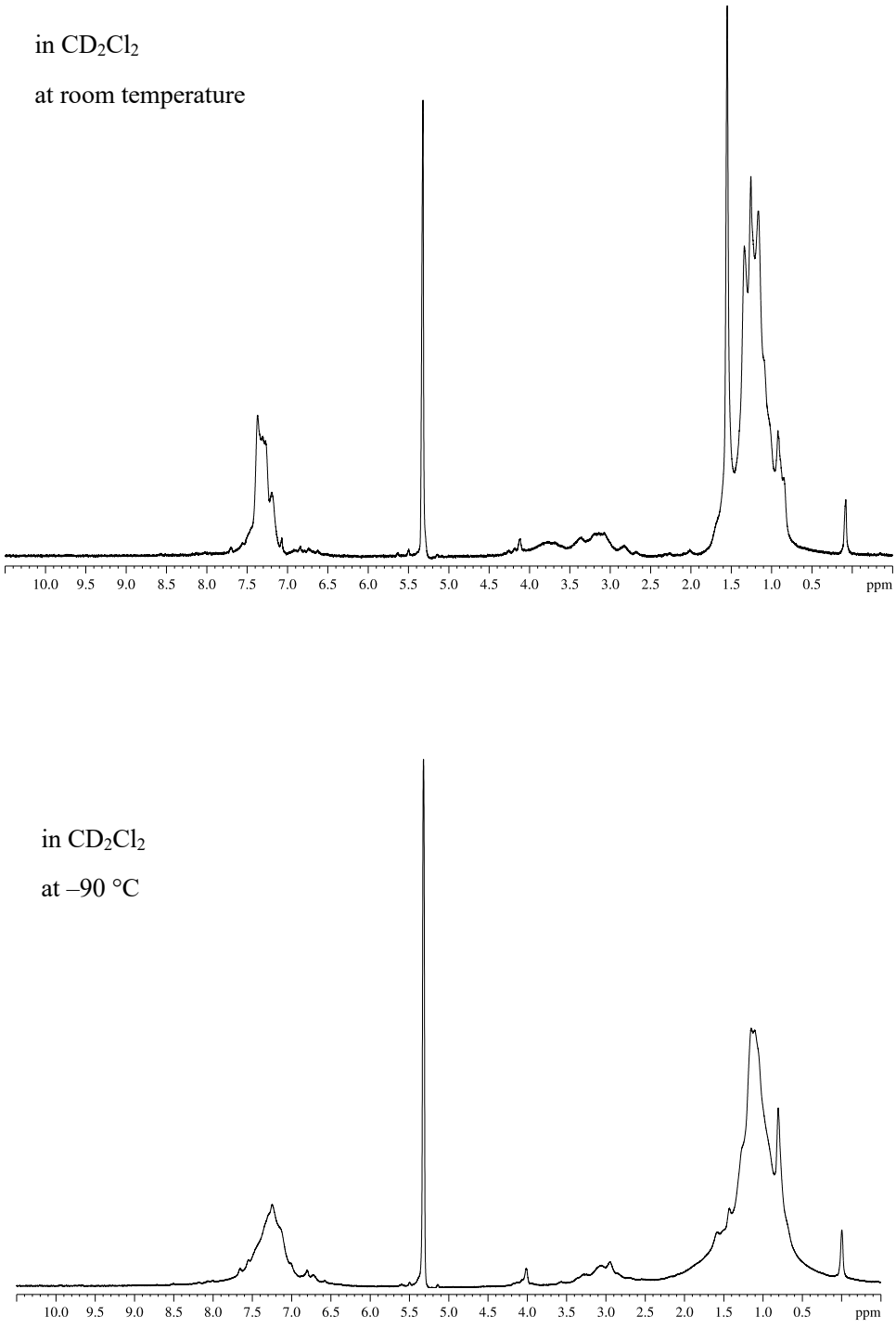

Supplementary Fig. 2. ^{1}H NMR spectra of **3** in CD_2Cl_2 at room temperature (top) and at –90 °C (bottom) (500 MHz).

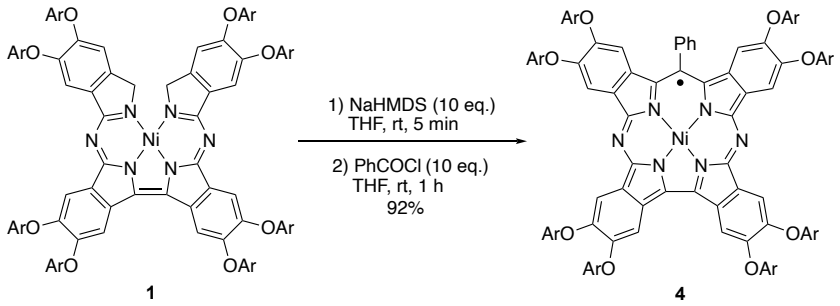

To a solution of **1** (10.0 mg, 5.11 μmol, 1.0 eq.) in THF (3 mL) was added NaHMDS (1.0 M in THF, 51 μL, 51 μmol, 10 eq.) at room temperature in a J-Young Schlenk flask in an Ar glovebox, and the dark brown solution was stirred at room temperature for 5 min. Then, to the solution was added benzoyl chloride (5.9 μL, 51 μmol, 10 eq.) at room temperature. The sealed flask was removed from the glovebox, and the brown solution was stirred at room temperature for 1 h. The solution was evaporated *in vacuo*. Column chromatography on silica gel using EtOAc/hexane (12:88) as an eluent gave the desired compound **4** as a brown solid (9.64 mg, 92%).

UV/vis/NIR ($CHCl_3$): λ_{max} ($\varepsilon \times 10^{-4}$) = 1665 (0.0542), 1345 (0.0532), 751 (1.40), 675 (0.855), 386 (5.24) nm.

IR (ATR): 2961, 1436, 1326, 1269, 1187, 1095, 880, 781 cm^{-1}.

HRMS (ESI): *m*/*z*: $[M]^+$ Calcd for $C_{135}H_{149}N_6NiO_8$ 2040.0785; Found 2040.0776.

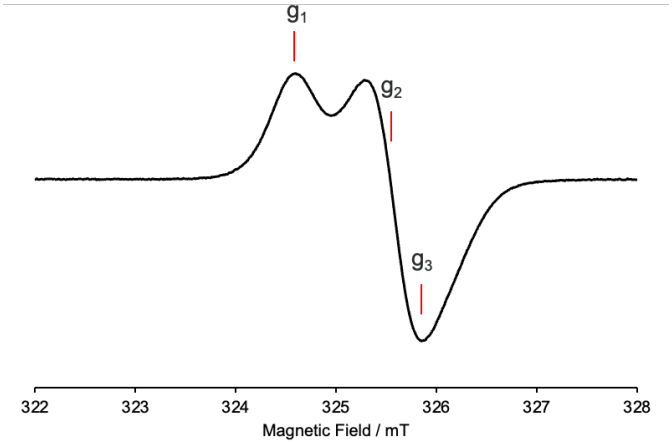

Supplementary Fig. 3. ESR spectrum of **4** in toluene at –150 °C (9125 MHz) (g_1 =2.0086, g_2 =2.0027, g_3 =2.0008).

in CD_2Cl_2

at room temperature

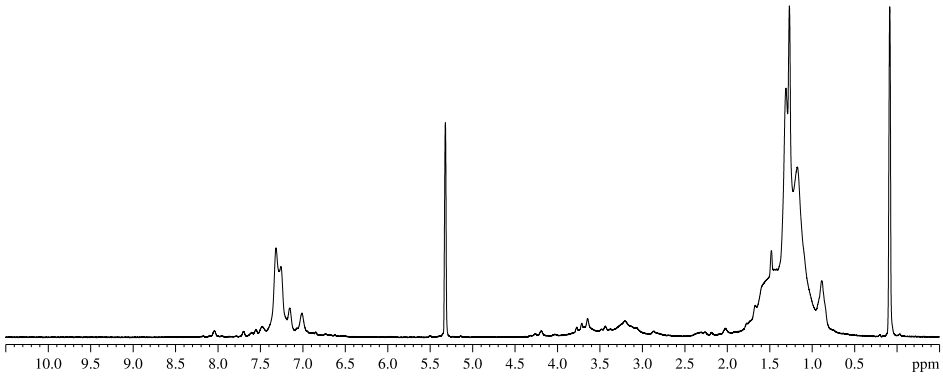

in CD_2Cl_2

at –90 °C

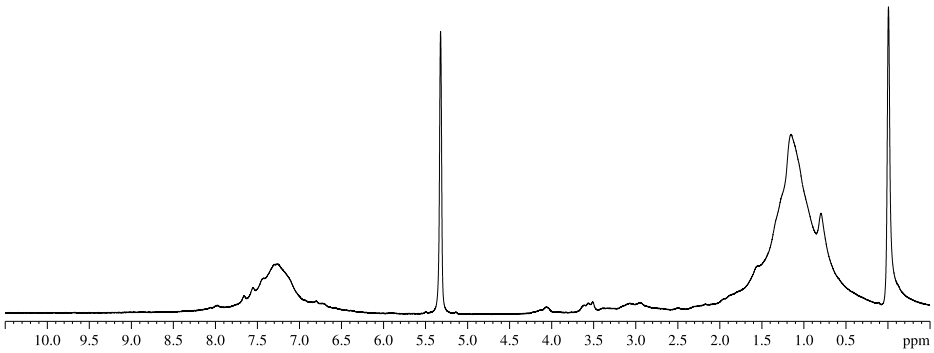

Supplementary Fig. 4. ^{1}H NMR spectra of **4** in CD_2Cl_2 at room temperature (top) and at –90 °C (bottom) (500 MHz).

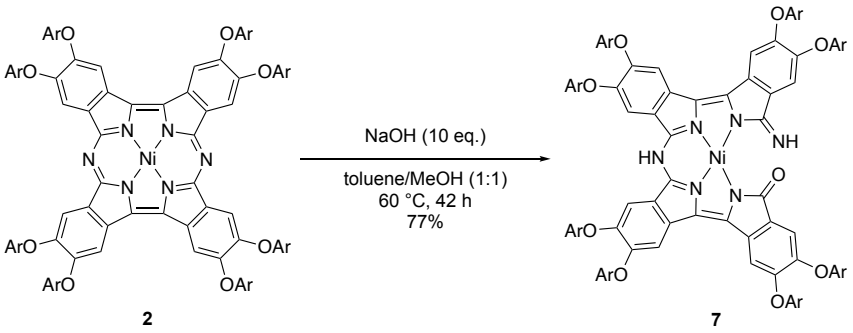

2 **7**

A mixture of **2** (15.8 mg, 8.09 μmol, 1.0 eq.) and NaOH (3.24 mg, 81.0 μmol, 10 eq.) in toluene (1 mL) and MeOH (1 mL) was stirred at 60 °C for 42 h. The blue solution was evaporated *in vacuo*. Column chromatography on silica gel using EtOAc/hexane (hexane only to 20:80) as an eluent gave the desired compound **7** as a blue solid (12.3 mg, 77%).

^{1}H-NMR (500 MHz, $CDCl_3$/TMS): δ 7.19–7.16 (m, 16H), 7.12–7.04 (m, 12H), 6.79 (s, 1H), 6.78 (s, 1H), 6.62 (s, 1H), 6.25 (s, 1H), 3.30–3.18 (m, 8H), 2.90–2.77 (m, 8H), 1.22–0.97 (m, 96H).

^{1}H-NMR (500 MHz, $CDCl_3$/DMSO-d_6 (1:1)): δ 12.27 (s, 1H, N–H, exchangeable with D_2O), 8.70 (brs, 1H, N–H, exchangeable with D_2O), 7.34–7.07 (m, 22H), 7.06–6.98 (m, 6H), 6.97 (s, 1H), 6.62 (s, 1H), 6.61 (s, 1H), 6.41 (s, 1H), 3.22–3.10 (m, 8H), 2.83–2.67 (m, 8H), 1.20–0.85 (m, 96H).

^{13}C-NMR (126 MHz, $CDCl_3$/TMS): δ 175.3, 163.2, 156.3, 155.6, 150.7, 150.6, 150.5, 150.4, 150.12, 150.06, 149.9, 149.8, 149.5, 149.1, 148.93, 148.87, 147.9, 147.6, 147.4, 147.1, 141.6, 141.5, 141.4, 140.7, 140.6, 140.5, 140.4, 138.3, 136.3, 132.3, 131.5, 130.9, 130.6, 129.0, 128.7, 127.5, 127.4, 126.8, 126.6, 126.2, 126.1, 126.0, 125.9, 125.55, 125.51, 124.8, 124.6, 124.5, 124.40, 124.36, 124.25, 124.21, 124.15, 111.4, 111.1, 110.8, 110.2, 108.6, 107.6, 107.1, 105.6, 27.43, 27.35, 27.3, 26.7, 26.65, 26.60, 26.5, 24.1, 23.9, 23.8, 23.7, 23.4, 23.3, 23.2, 23.1.

UV/vis/NIR ($CHCl_3$): λ_{max} (ε × 10^{-4}) = 617 (0.815), 420 (3.97) nm.

IR (ATR): 2962, 1684, 1606, 1541, 1436, 1362, 1325, 1277, 1215, 893, 779 cm^{-1}.

HRMS (ESI): *m*/*z*: $[M+H]^+$ Calcd for $C_{128}H_{147}N_6NiO_9$ 1970.0577; Found 1970.0570.

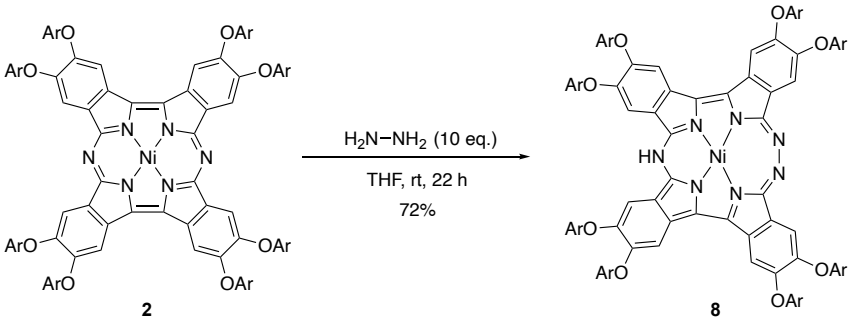

2 **8**

To a solution of **2** (8.34 mg, 4.27 μmol, 1.0 eq.) in THF (2 mL) was added hydrazine (1.4 μL, 43 μmol, 10 eq.), and the solution was stirred at room temperature for 22 h. The green solution was evaporated *in vacuo*. Column chromatography on silica gel using EtOAc/hexane (hexane only to 20:80) as an

eluent gave the desired compound **8** as a green solid (6.09 mg, 72%).

^{1}H-NMR (500 MHz, $CDCl_3$/TMS): δ 7.97 (s, 2H), 7.921 (s, 2H), 7.916 (s, 2H), 7.53 (s, 2H), 7.39–7.27 (m, 18H), 7.24–7.21 (m, 6H), 3.50–3.41 (m, 8H), 3.12 (sept, 4H, J = 7.0 Hz), 3.00 (sept, 4H, J = 7.0 Hz), 1.30–1.04 (m, 96H).

^{13}C-NMR (126 MHz, $CDCl_3$/TMS): δ 151.1, 150.9, 149.9, 149.8, 149.6, 148.5, 148.3, 147.8, 144.8, 142.0, 141.9, 141.1, 140.7, 133.0, 128.8, 127.5, 126.6, 126.3, 125.84, 125.79, 125.1, 124.8, 124.5, 124.4, 124.2, 111.1, 110.8, 107.7, 106.2, 27.8, 27.6, 27.1, 26.9, 24.4, 24.1, 24.0, 23.5, 23.1.

UV/vis/NIR ($CHCl_3$): λ_{max} ($\varepsilon \times 10^{-4}$) = 649 (0.657), 596 (0.328), 419 (2.75) nm.

IR (ATR): 2960, 1453, 1325, 1278, 1178, 1095, 779, 670 cm^{-1}.

HRMS (ESI): *m/z*: $[M+H]^+$ Calcd for $C_{128}H_{146}N_7NiO_8$ 1967.0581; Found 1967.0566.

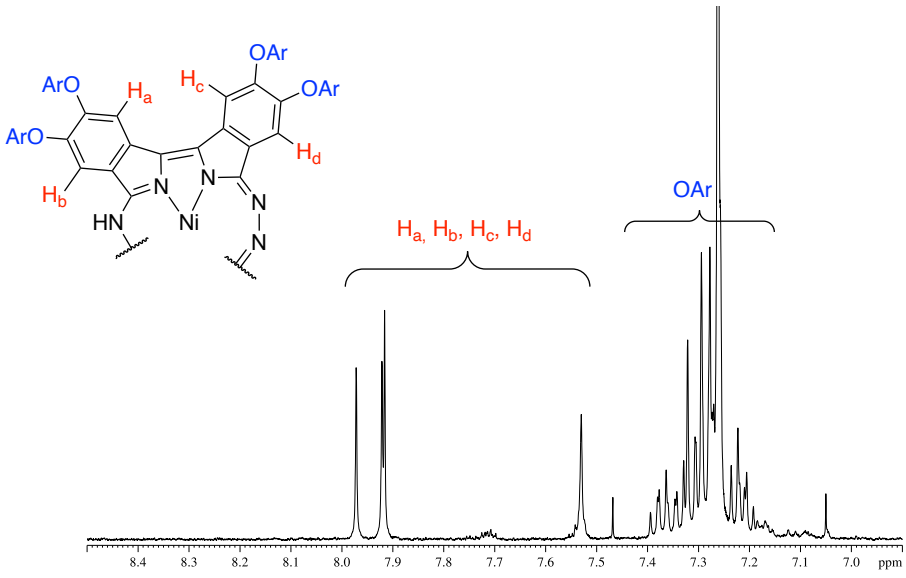

Supplementary Fig. 5. Partial ^{1}H NMR spectrum of **8** in $CDCl_3$ (500 MHz).

2-2. Screening of Reaction Conditions for Tetramerization

Base (0.5 mmol, 1.0 eq.) in dodecanethiol (1.0 mL) was stirred at 100 °C for 5 min. Then, to the mixture was added phthalonitrile **6** (0.5 mmol, 1.0 eq.). The mixture was stirred at 100 °C for x h and 180 °C for y h. The black suspension was quenched with $NaHCO_3$ aq., extracted with $CHCl_3$ three times, washed with water, and evaporated *in vacuo*. The yields of **5**, phthalocyanine **S1**,[1] and phthalonitrile trimer **S2**[2] were determined by ^1H NMR analysis in $CDCl_3$ using 1,1,2,2-tetrachloroethane as an internal standard.

Supplementary Table 1. Screening of reaction conditions for synthesis of **5**.

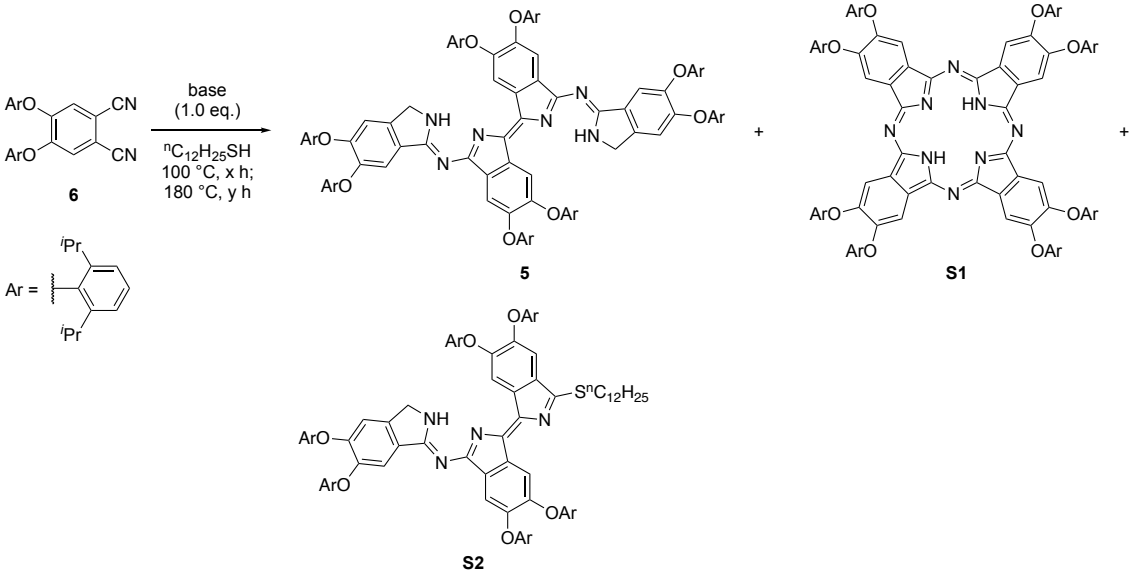

entry	base	x	y	yield [%][a] 5	S1	S2	selectivity ([5]:[S1])
1	Na	0	2	6	17	3	26:74
2	Na	1	1	19	9	5	68:32
3	Na	1	3	3	10	3	23:77
4	Na	2	1	21	6	3	78:22
5[b]	Na	2	1	4	23	2	15:85
6	Li	2	1	7	5	2	58:42
7	NaH	2	1	20	14	4	59:41
8	KH	2	1	24	6	6	80:20
9	Cs_2CO_3	2	1	32	3	2	91:9

[a] Determined by ^1H NMR. [b] Na (5 eq.) was used.

2-3. Formation of Antiaromatic Macrocycle 2

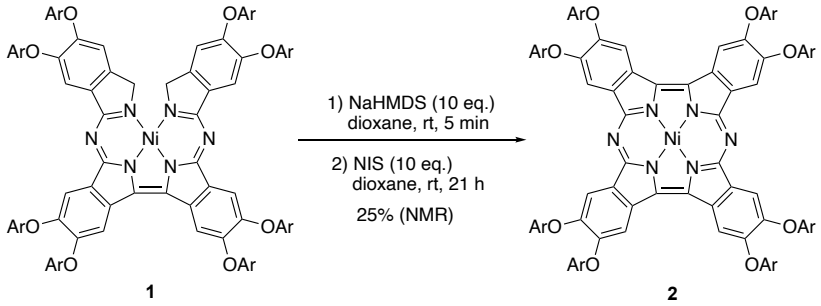

Supplementary Fig. 6. Cyclization of **1** with NIS.

To a solution of **1** (1.8 mg, 0.92 μmol, 1.0 eq.) in 1,4-dioxane (0.3 mL) was added NaHMDS (1.0 M in THF, 9.2 μL, 9.2 μmol, 10 eq.) at room temperature in a J-Young NMR tube in an Ar glovebox, and the dark brown solution was left standing at room temperature for 5 min. Then, to the solution was added a suspension of *N*-iodosuccinimide (2.1 mg, 9.3 μmol, 10 eq.) in 1,4-dioxane (0.3 mL) at room temperature. The sealed NMR tube was removed from the glovebox, and the brown solution was left standing at room temperature for 21 h. The solution was evaporated *in vacuo*. The yield (25%) of **2** was determined by ^{1}H NMR analysis in $CDCl_3$ using 1,1,2,2-tetrachloroethane as an internal standard.

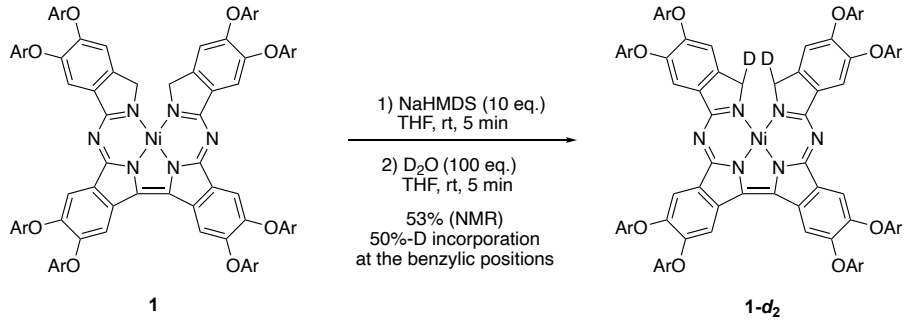

Supplementary Fig. 7. Deuteration of **1** with NaHMDS and D_2O.

To a solution of **1** (2.0 mg, 1.0 μmol, 1.0 eq.) in THF (0.6 mL) was added sodium hexamethyldisilazide (1.0 M in THF, 10 μL, 10 μmol, 10 eq.) at room temperature in a J-Young NMR tube in an Ar glovebox, and the dark brown solution was left standing at room temperature for 5 min. The sealed NMR tube was removed from the glovebox, and to the solution was added D_2O (1.8 μL, 100 μmol, 100 eq.) in an Ar bag. Then the red solution was left standing at room temperature for 5 min, and was evaporated *in vacuo*. The yield (53%) of **1-*d*$_2$** was determined by ^{1}H NMR analysis in $CDCl_3$ using 1,1,2,2-tetrachloroethane as an internal standard. The deuterium incorporation (50%D) at the benzylic positions was determined by ^{1}H NMR analysis in $CDCl_3$ based on the integration of the isoindoline unit as the reference (2.00H).

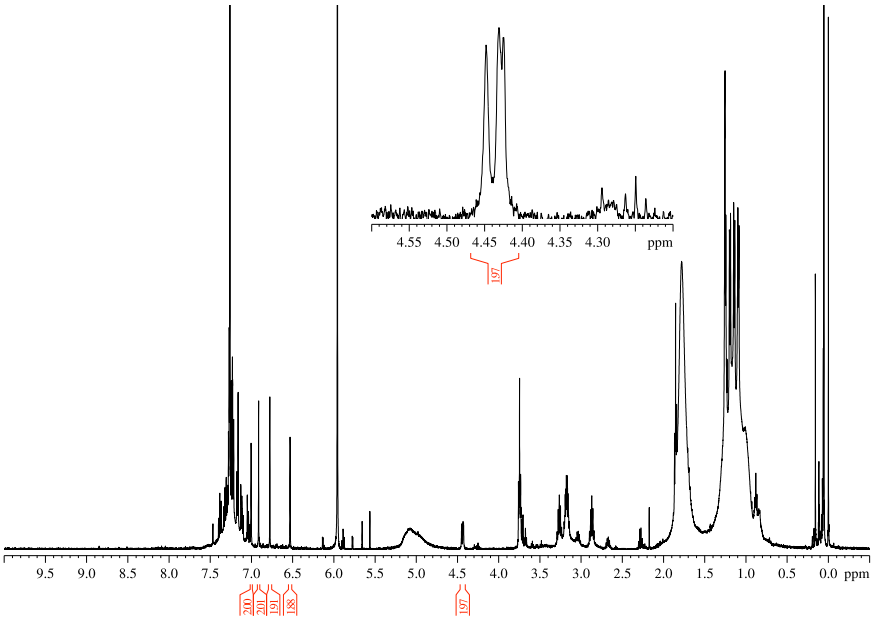

Supplementary Fig. 8. Crude ^{1}H NMR spectrum of **1-*d*$_2$** in $CDCl_3$ (500 MHz).

2-4. Redox Reactions of Radicals 3 and 4

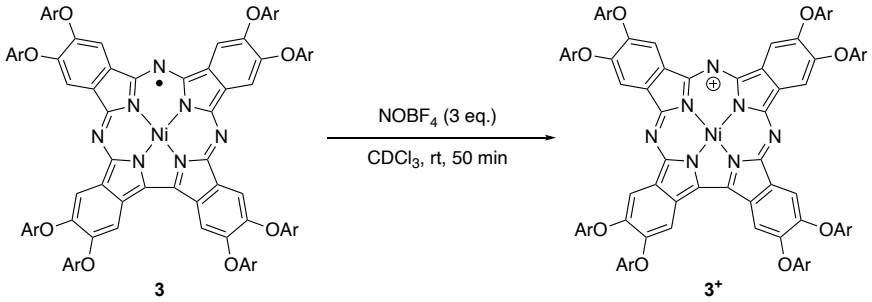

To a solution of **3** (1.8 mg, 0.91 μmol, 1 eq.) in $CDCl_3$ (0.6 mL) was added $NOBF_4$ (0.3 mg, 3 μmol, 3 eq.) at room temperature in a J-Young NMR tube in an Ar glovebox. The sealed NMR tube was removed from the glovebox, and left standing at room temperature for 50 min. The ^1H NMR measurement suggested the formation of 16π-electron antiaromatic species $\mathbf{3}^+$, judging from the four aromatic singlets (6.30–6.17 ppm) observed in an upfield region.

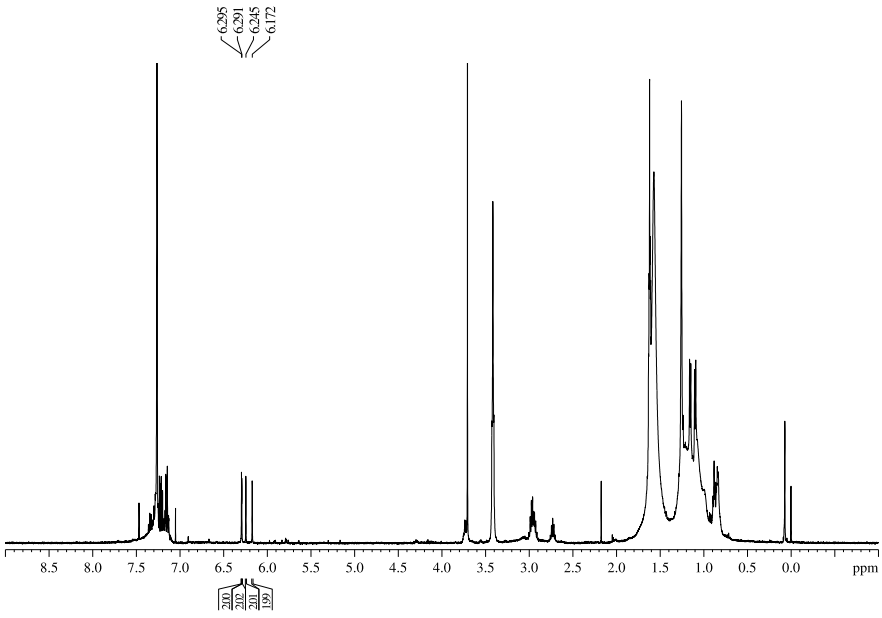

Supplementary Fig. 9. In-situ ^1H NMR spectrum of $\mathbf{3}^+$ in $CDCl_3$ (500 MHz).

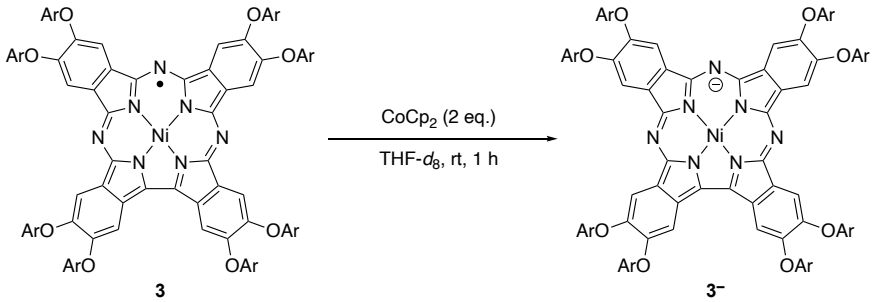

To a solution of **3** (2.0 mg, 1.0 μmol, 1 eq.) in THF-d_8 (0.6 mL) was added $CoCp_2$ (0.3 mg, 2 μmol, 2 eq.) at room temperature in a J-Young NMR tube in an Ar glovebox. The sealed NMR tube was removed from the glovebox, and left standing at room temperature for 1 h. The ^{1}H NMR measurement suggested the formation of 18π-electron aromatic species **3**$^-$, judging from the four aromatic singlets (8.11–8.01 ppm) observed in a downfield region.

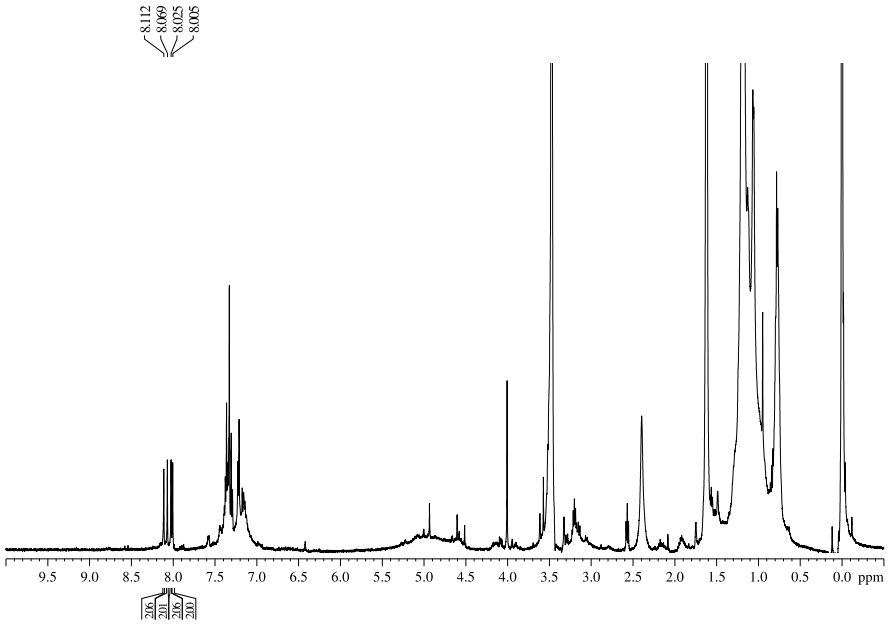

Supplementary Fig. 10. In-situ ^{1}H NMR spectrum of **3**$^-$ in THF-d_8 (500 MHz).

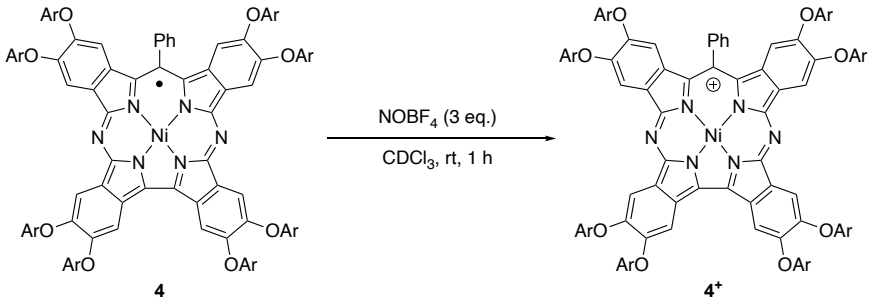

To a solution of **4** (2.0 mg, 0.98 μmol, 1 eq.) in $CDCl_3$ (0.6 mL) was added $NOBF_4$ (0.4 mg, 3 μmol, 3 eq.) at room temperature in a J-Young NMR tube in an Ar glovebox. The sealed NMR tube was removed from the glovebox, and left standing at room temperature for 1 h. The ^{1}H NMR measurement suggested the formation of 16π-electron antiaromatic species $\mathbf{4}^+$, judging from the four aromatic singlets (5.93–3.94 ppm) observed in an upfield region.

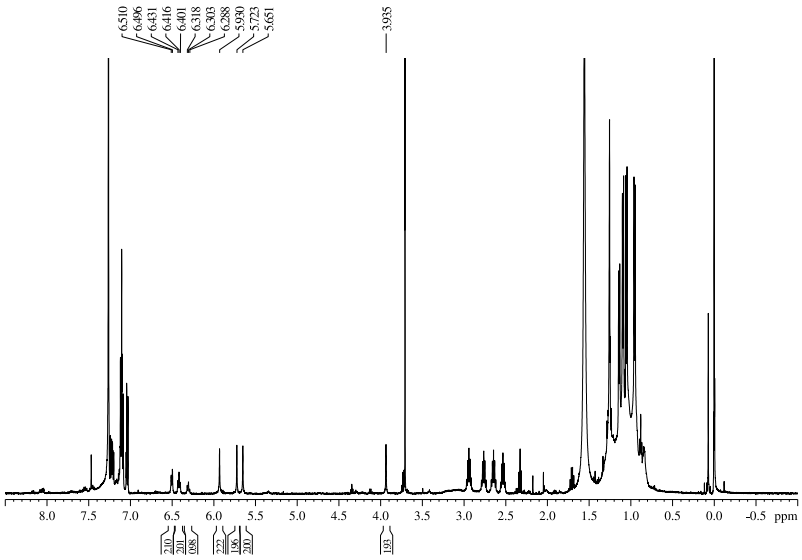

Supplementary Fig. 11. In-situ ^{1}H NMR spectrum of $\mathbf{4}^+$ in $CDCl_3$ (500 MHz).

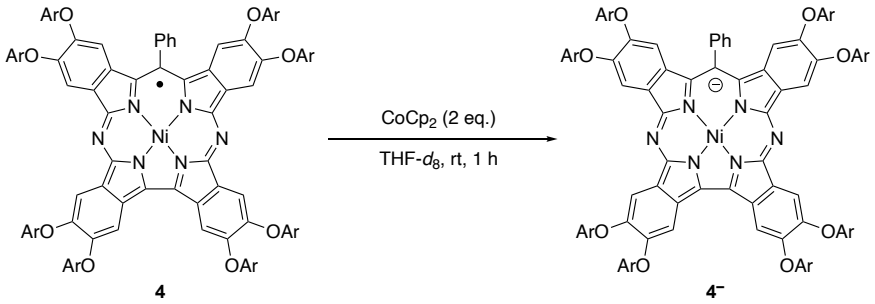

To a solution of **4** (2.0 mg, 0.98 μmol, 1 eq.) in THF-d_8 (0.6 mL) was added $CoCp_2$ (0.3 mg, 2 μmol, 2 eq.) at room temperature in a J-Young NMR tube in an Ar glovebox. The sealed NMR tube was removed from the glovebox, and left standing at room temperature for 1 h. The ^{1}H NMR measurement suggested the formation of 18π-electron aromatic species **4**$^-$, judging from the three aromatic singlets (8.14, 8.11, 7.94 ppm) observed in a downfield region. One aromatic singlet was observed in an upfield region (5.88 ppm) because of a ring current effect of the Ph group attached to the *meso*-position.

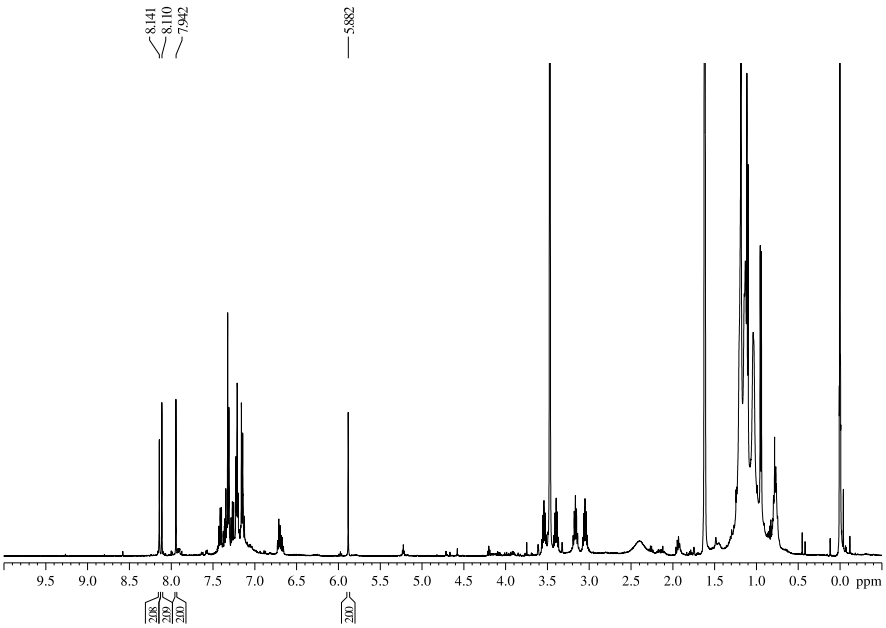

Supplementary Fig. 12. In-situ ^{1}H NMR spectrum of **4**$^-$ in THF-d_8 (500 MHz).

3. Physicochemical Properties

3-1. X-ray Diffraction Analysis

A single crystal in immersion oil was mounted on a Rigaku XtaLAB Synergy-S diffractometer with a HyPix-6000HE HPC detector. The diffraction data were collected using Cu *K*α radiation under a cold nitrogen stream at 123 K (**1**, **3**, **4**, **7**), 100 K (**8**), or 93 K (**2**). The images were processed with the Rigaku CrysAlis^{PRO} software. The structure was solved by a direct method and refined on F^2 by a least-squares method by the programs SHELXT2015[3] and SHELXL2015,[4] respectively. All the non-hydrogen atoms were refined anisotropically. All the hydrogen atoms were put on the calculated geometry and refined by applying riding models. Disordered solvent molecules was removed by the solvent masking procedure using Olex2 software.[5] Disordered 2,6-diisopropylphenoxy groups were fixed by using the DFIX, AFIX, DANG, SADI, RIGU, and SIMU restriction commands available for SHELXL.

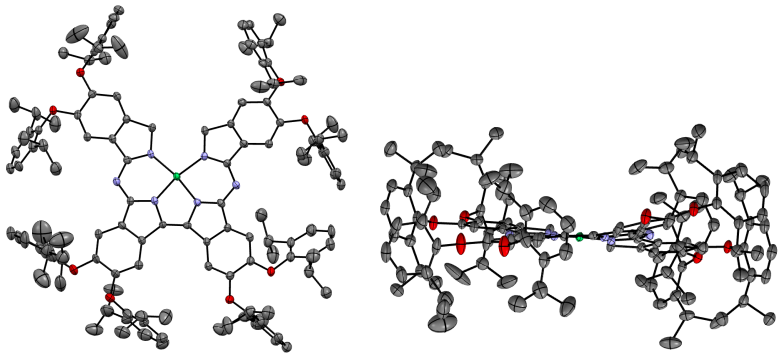

Supplementary Fig. 13. X-ray structure of **1** (left: top view, right: side view) (CCDC 2382224). Thermal ellipsoids are set at 30% probability. H atoms and solvent molecules (pyridine) are omitted for clarity. One of the two molecules in the unit cell is shown.

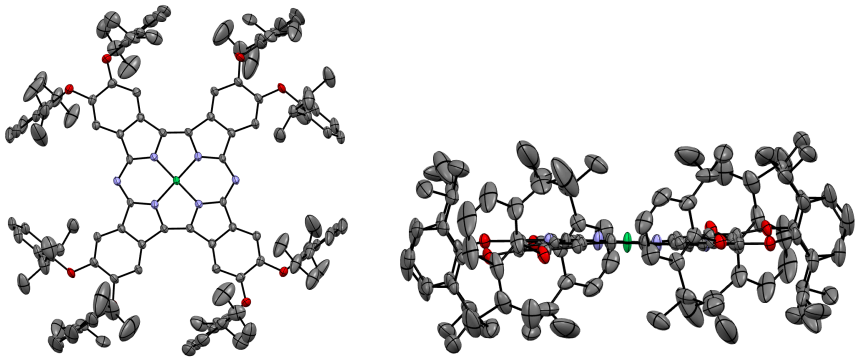

Supplementary Fig. 14. X-ray structure of **2** (left: top view, right: side view) (CCDC 2382225). Thermal ellipsoids are set at 30% probability. H atoms are omitted for clarity. One of the two molecules in the unit cell is shown.

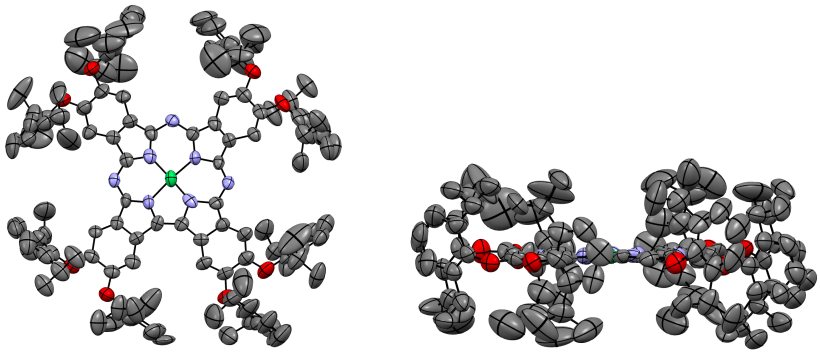

Supplementary Fig. 15. X-ray structure of **3** (left: top view, right: side view) (CCDC 2382226). Thermal ellipsoids are set at 30% probability. H atoms are omitted for clarity. One of the two molecules in the unit cell is shown.

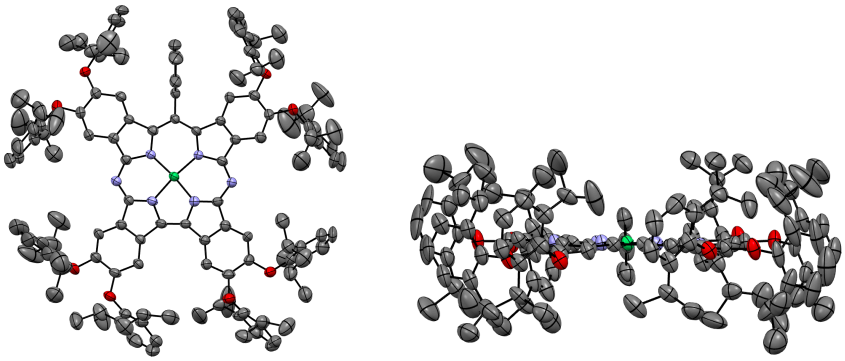

Supplementary Fig. 16. X-ray structure of **4** (left: top view, right: side view) (CCDC 2382227). Thermal ellipsoids are set at 30% probability. H atoms are omitted for clarity. One of the two molecules in the unit cell is shown.

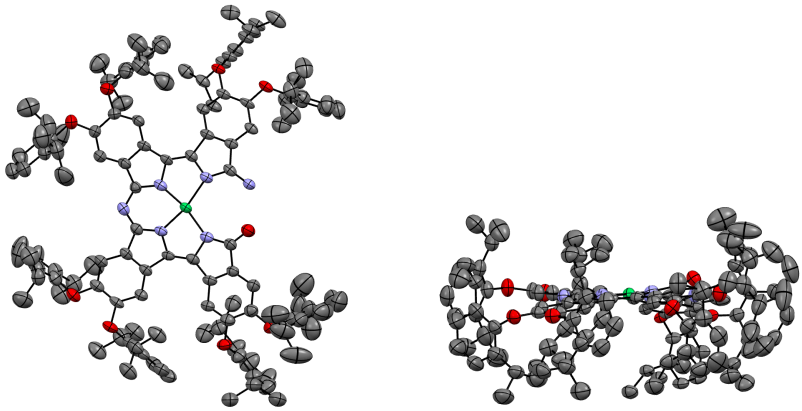

Supplementary Fig. 17. X-ray structure of **7** (left: top view, right: side view) (CCDC 2416449). Thermal ellipsoids are set at 30% probability. H atoms are omitted for clarity. One of the two molecules in the unit cell is shown.

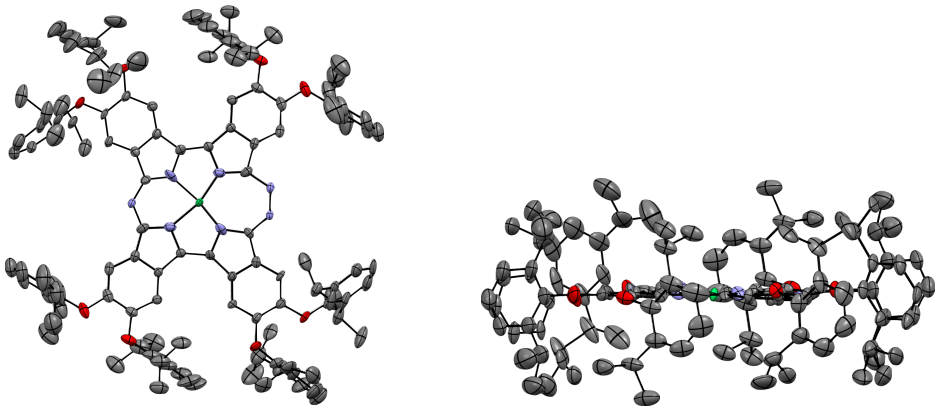

Supplementary Fig. 18. X-ray structure of **8** (left: top view, right: side view) (CCDC 2382228). Thermal ellipsoids are set at 30% probability. H atoms are omitted for clarity. One of the two disordered molecules in the unit cell is shown.

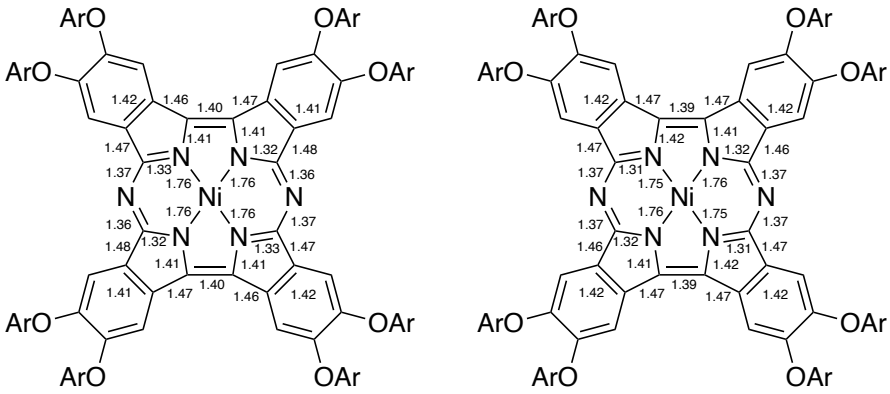

Supplementary Fig. 19. Selected bond lengths (Å) in the crystal of **2**. Two molecules in the unit cell are shown.

Supplementary Table 2. Summary of X-ray data for **1** and **2**.

Compound	**1**	**2**
Solvent for recrystallization	pyridine/MeOH (vapor diffusion)	acetone/MeOH (vapor diffusion)
Formula	$2(C_{128}H_{148}N_6NiO_8)$, $2(C_5H_5N)$	$2(C_{64}H_{72}N_3Ni_{0.5}O_4)$
Formula weight	4072.65	1953.19
Crystal system	Triclinic	Triclinic
Space group	$P\ \bar{1}$	$P\ \bar{1}$
Crystal size (mm)	0.1×0.067×0.062	0.134×0.093×0.073
Crystal color and shape	Red plate	Dark yellow plate
Wavelength (Å)	1.54184	1.54184
a (Å)	17.5619(2)	16.8796(4)
b (Å)	17.6582(2)	18.7821(5)
c (Å)	39.9112(7)	20.5996(6)
α (°)	97.2430(10)	65.183(3)
β (°)	97.2880(10)	83.181(2)
γ (°)	90.2630(10)	89.791(2)
Volume (Å)	12176.3(3)	5878.0(3)
Z	2	2
$\rho_{calcd.}$ (g cm^{-3})	1.111	1.104
μ (mm^{-1})	0.672	0.675
θ_{min}, θ_{max} (°)	2.610, 60.696	2.557, 72.427
No. of reflection (unique)	128319 (35182)	73013 (23539)
R_{int}	0.0809	0.0516
Completeness to θ (%)	94.6	98.9
Goodness-of-fit on F^2	1.047	1.027
Final R_1 and wR_2 indices $[I > 2\sigma(I)]$	0.1077, 0.2768	0.0970, 0.2505
R_1 and wR_2 indices (all data)	0.1481, 0.3002	0.1305, 0.2751
CCDC number	2382224	2382225

Supplementary Table 3. Summary of X-ray data for **3** and **4**.

Compound	**3**	**4**
Solvent for recrystallization	1-iodo-3,5-bis(trifluoromethyl)benzene/MeOH (vapor diffusion)	2-iodotoluene/MeOH (vapor diffusion)
Formula	$2(C_{128}H_{144}N_7NiO_8)$	$2(C_{135}H_{149}N_6NiO_8)$
Formula weight	3934.41	4084.61
Crystal system	Triclinic	Triclinic
Space group	*P* 1	$P\ \bar{1}$
Crystal size (mm)	0.10×0.05×0.04	0.170×0.053×0.047
Crystal color and shape	Black needle	Green block
Wavelength (Å)	1.54184	1.54184
a (Å)	16.8147(5)	21.1782(4)
b (Å)	18.3978(8)	24.7876(5)
c (Å)	21.3290(12)	25.4002(4)
α (°)	114.742(5)	97.9363(14)
β (°)	96.345(4)	104.6434(14)
γ (°)	90.973(3)	93.7027(15)
Volume (Å)	5941.2(5)	12708.3(4)
Z	1	2
$\rho_{calcd.}$ (g cm^{-3})	1.100	1.067
μ (mm^{-1})	0.673	0.644
θ_{min}, θ_{max} (°)	2.626, 64.967	2.415, 59.087
No. of reflection (unique)	84231 (32152)	255252 (37635)
R_{int}	0.1489	0.1747
Completeness to θ (%)	99.6	96.1
Goodness-of-fit on F^2	0.907	1.136
Final R_1 and wR_2 indices [$I > 2\sigma(I)$]	0.0991, 0.2625	0.1152, 0.3292
R_1 and wR_2 indices (all data)	0.2231, 0.3608	0.1856, 0.3701
CCDC number	2382226	2382227

Supplementary Table 4. Summary of X-ray data for **7** and **8**.

Compound	**7**	**8**
Solvent for recrystallization	acetone/MeOH (vapor diffusion)	1-iodo-3,5-bis(trifluoromethyl)benzene/MeOH (vapor diffusion)
Formula	$2(C_{128}H_{146}N_6NiO_9)$	$2(C_{64}H_{72.5}N_{3.5}Ni_{0.5}O_4)$
Formula weight	3942.42	1968.21
Crystal system	Triclinic	Monoclinic
Space group	$P\ \bar{1}$	$P\ 2_1/c$
Crystal size (mm)	0.246×0.133×0.046	0.21×0.13×0.03
Crystal color and shape	Green plate	Black block
Wavelength (Å)	1.54184	1.54184
a (Å)	21.7626(4)	16.6870(4)
b (Å)	21.9239(3)	18.9466(5)
c (Å)	28.9796(3)	38.0755(11
α (°)	90.0590(10)	90
β (°)	109.6050(10)	100.209(3)
γ (°)	109.280(2)	90
Volume (Å)	12197.1(3)	11847.4(6)
Z	2	4
$\rho_{calcd.}$ (g cm^{-3})	1.073	1.103
μ (mm^{-1})	0.660	0.675
θ_{min}, θ_{max} (°)	2.506, 72.390	2.662, 68.739
No. of reflection (unique)	148456 (46729)	87165 (24048)
R_{int}	0.0660	0.0307
Completeness to θ (%)	97.9	99.7
Goodness-of-fit on F^2	1.748	1.662
Final R_1 and wR_2 indices [$I > 2\sigma(I)$]	0.1471, 0.4159	0.1301, 0.4030
R_1 and wR_2 indices (all data)	0.1686, 0.4329	0.1521, 0.4182
CCDC number	2416449	2382228

Notes on CheckCif file B-level alerts

Compound **1**

```
THETM01_ALERT_3_B  The value of sine(theta_max)/wavelength is less than 0.575
           Calculated sin(theta_max)/wavelength =    0.5670
```

Author Response: The quality of the crystal was low probably due to its small size. The crystal under investigation showed no significant diffraction intensity beyond a certain resolution limit.

```
PLAT029_ALERT_3_B _diffrn_measured_fraction_theta_full value Low .      0.946 Why?
```

Author Response: The crystal was weakly diffracting. Thus, low completeness was obtained due to incomplete coverage of the diffraction patterns.

```
PLAT220_ALERT_2_B NonSolvent   Resd 1  C   Ueq(max)/Ueq(min) Range        7.5 Ratio
PLAT220_ALERT_2_B NonSolvent   Resd 2  C   Ueq(max)/Ueq(min) Range        6.8 Ratio
```

Author Response: These results are due to unresolvable disorders derived from limited resolution of the crystal data.

```
PLAT242_ALERT_2_B Low    'MainMol' Ueq as Compared to Neighbors of        C045 Check
PLAT242_ALERT_2_B Low    'MainMol' Ueq as Compared to Neighbors of        C04D Check
```

Author Response: These results are due to large disorders derived from the flexibility of the peripheral 2,6-diisopropylphenoxy groups.

```
PLAT360_ALERT_2_B Short  C(sp3)-C(sp3) Bond  C07Q     - C088     .        1.32 Ang.
PLAT412_ALERT_2_B Short Intra XH3 .. XHn     H07R     ..H08O     .        1.76 Ang.
                                                      x,y,z  =      1_555 Check
```

Author Response: These results are due to low quality of the crystal data. Also, the unresolved thermal disorder can affect the H...H distances.

Compound **2**

```
PLAT213_ALERT_2_B Atom C03J            has ADP max/min Ratio .....        4.1 prolat
```

Author Response: There is a large amount of disorder in the structure.

```
PLAT220_ALERT_2_B NonSolvent   Resd 1  C   Ueq(max)/Ueq(min) Range        6.5 Ratio
PLAT220_ALERT_2_B NonSolvent   Resd 2  C   Ueq(max)/Ueq(min) Range        8.1 Ratio
```

Author Response: These results are due to unresolvable disorders in the crystal data.

```
PLAT241_ALERT_2_B High   'MainMol' Ueq as Compared to Neighbors of         C48 Check
PLAT242_ALERT_2_B Low    'MainMol' Ueq as Compared to Neighbors of        C03M Check
PLAT242_ALERT_2_B Low    'MainMol' Ueq as Compared to Neighbors of        C029 Check
PLAT242_ALERT_2_B Low   'MainMol' Ueq as Compared to Neighbors of         C035 Check
```

Author Response: These results are due to large disorders derived from the flexibility of the peripheral 2,6-diisopropylphenoxy groups.

```
PLAT360_ALERT_2_B Short  C(sp3)-C(sp3) Bond  C42      - C03M     .        1.30 Ang.
```

Author Response: This result is due to low quality of the crystal data.

Compound **3**

```
PLAT026_ALERT_3_B Ratio Observed / Unique Reflections (too) Low ..        30% Check
PLAT084_ALERT_3_B High wR2 Value (i.e. > 0.25) ..................      0.36 Report
```

Author Response: The quality of the crystal was low probably due to its small size. The crystal under investigation showed no significant diffraction intensity beyond a certain resolution limit.

```
PLAT213_ALERT_2_B Atom C91            has ADP max/min Ratio .....        4.1 prolat
```

Author Response: There is a large amount of disorder in the structure.

```
 PLAT220_ALERT_2_B NonSolvent  Resd 1  C   Ueq(max)/Ueq(min) Range        6.1 Ratio
PLAT220_ALERT_2_B NonSolvent   Resd 2  C   Ueq(max)/Ueq(min) Range        6.2 Ratio
```

Author Response: These results are due to unresolvable disorders in the crystal data.

```
PLAT241_ALERT_2_B High   'MainMol' Ueq as Compared to Neighbors of         C8 Check
PLAT241_ALERT_2_B High   'MainMol' Ueq as Compared to Neighbors of        C27 Check
PLAT241_ALERT_2_B High   'MainMol' Ueq as Compared to Neighbors of       C03B Check
PLAT241_ALERT_2_B High   'MainMol' Ueq as Compared to Neighbors of        C17 Check
PLAT241_ALERT_2_B High   'MainMol' Ueq as Compared to Neighbors of        C37 Check
PLAT241_ALERT_2_B High   'MainMol' Ueq as Compared to Neighbors of       C04I Check
PLAT242_ALERT_2_B Low    'MainMol' Ueq as Compared to Neighbors of         C4 Check
PLAT242_ALERT_2_B Low    'MainMol' Ueq as Compared to Neighbors of        C42 Check
PLAT242_ALERT_2_B Low    'MainMol' Ueq as Compared to Neighbors of        C46 Check
PLAT242_ALERT_2_B Low    'MainMol' Ueq as Compared to Neighbors of       C021 Check
PLAT242_ALERT_2_B Low    'MainMol' Ueq as Compared to Neighbors of       C026 Check
PLAT242_ALERT_2_B Low    'MainMol' Ueq as Compared to Neighbors of        C57 Check
PLAT242_ALERT_2_B Low    'MainMol' Ueq as Compared to Neighbors of        C69 Check
PLAT242_ALERT_2_B Low    'MainMol' Ueq as Compared to Neighbors of       C041 Check
PLAT242_ALERT_2_B Low    'MainMol' Ueq as Compared to Neighbors of       C043 Check
PLAT242_ALERT_2_B Low    'MainMol' Ueq as Compared to Neighbors of        C14 Check
PLAT242_ALERT_2_B Low    'MainMol' Ueq as Compared to Neighbors of       C027 Check
PLAT242_ALERT_2_B Low    'MainMol' Ueq as Compared to Neighbors of        C59 Check
PLAT242_ALERT_2_B Low    'MainMol' Ueq as Compared to Neighbors of        C60 Check
PLAT242_ALERT_2_B Low    'MainMol' Ueq as Compared to Neighbors of        C66 Check
PLAT242_ALERT_2_B Low    'MainMol' Ueq as Compared to Neighbors of        C75 Check
PLAT242_ALERT_2_B Low    'MainMol' Ueq as Compared to Neighbors of       C050 Check
PLAT242_ALERT_2_B Low    'MainMol' Ueq as Compared to Neighbors of       C051 Check
PLAT242_ALERT_2_B Low    'MainMol' Ueq as Compared to Neighbors of       C05N Check
```

Author Response: These results are due to large disorders derived from the flexibility of the peripheral 2,6-diisopropylphenoxy groups.

```
PLAT334_ALERT_2_B Small <C-C> Benzene Dist.   C009                      1.34 Ang.
PLAT341_ALERT_3_B Low Bond Precision on  C-C Bonds ..............   0.03592 Ang.
PLAT360_ALERT_2_B Short  C(sp3)-C(sp3) Bond  C34      -               1.26 Ang.
PLAT363_ALERT_2_B Long   C(sp3)-C(sp2) Bond  C42      -               1.74 Ang.
PLAT915_ALERT_3_B No Flack x Check Done: Low Friedel Pair Coverage       31 %
```

Author Response: These results are a consequence of large thermal disorders due to low quality of the crystal data.

Compound **4**

```
THETM01_ALERT_3_B  The value of sine(theta_max)/wavelength is less than 0.575
           Calculated sin(theta_max)/wavelength =    0.5688
PLAT084_ALERT_3_B High wR2 Value (i.e. > 0.25) ...................       0.37 Report
```

Author Response: The quality of the crystal was low probably due to its small size. The crystal under investigation showed no significant diffraction intensity beyond a certain resolution limit.

```
PLAT220_ALERT_2_B NonSolvent   Resd 1  C   Ueq(max)/Ueq(min) Range         6.9 Ratio
PLAT220_ALERT_2_B NonSolvent   Resd 2  C   Ueq(max)/Ueq(min) Range         7.0 Ratio
```

Author Response: These results are due to unresolvable disorders in the crystal data.

```
PLAT241_ALERT_2_B High   'MainMol' Ueq as Compared to Neighbors of       C159 Check
PLAT241_ALERT_2_B High   'MainMol' Ueq as Compared to Neighbors of       C319 Check
PLAT242_ALERT_2_B Low    'MainMol' Ueq as Compared to Neighbors of        C50 Check
PLAT242_ALERT_2_B Low    'MainMol' Ueq as Compared to Neighbors of        C99 Check
PLAT242_ALERT_2_B Low    'MainMol' Ueq as Compared to Neighbors of       C113 Check
PLAT242_ALERT_2_B Low    'MainMol' Ueq as Compared to Neighbors of       C187 Check
PLAT242_ALERT_2_B Low    'MainMol' Ueq as Compared to Neighbors of       C260 Check
PLAT242_ALERT_2_B Low    'MainMol' Ueq as Compared to Neighbors of        O86 Check
PLAT242_ALERT_2_B Low    'MainMol' Ueq as Compared to Neighbors of       C132 Check
PLAT242_ALERT_2_B Low    'MainMol' Ueq as Compared to Neighbors of       C139 Check
PLAT242_ALERT_2_B Low    'MainMol' Ueq as Compared to Neighbors of       C142 Check
PLAT242_ALERT_2_B Low    'MainMol' Ueq as Compared to Neighbors of       C169 Check
PLAT242_ALERT_2_B Low    'MainMol' Ueq as Compared to Neighbors of       C194 Check
PLAT242_ALERT_2_B Low    'MainMol' Ueq as Compared to Neighbors of       C233 Check
PLAT242_ALERT_2_B Low    'MainMol' Ueq as Compared to Neighbors of       C247 Check
```

Author Response: These results are due to large disorders derived from the flexibility of the peripheral 2,6-diisopropylphenoxy groups.

```
PLAT341_ALERT_3_B Low Bond Precision on  C-C Bonds ...............     0.0155 Ang.
```

Author Response: This is a result of limited data quality.

```
PLAT413_ALERT_2_B Short Inter XH3 .. XHn     H21G     ..H29F     .       1.92 Ang.
                                             x,y,z  =      1_555 Check
PLAT413_ALERT_2_B Short Inter XH3 .. XHn     H21H     ..H29F     .       1.90 Ang.
                                             x,y,z  =      1_555 Check
PLAT413_ALERT_2_B Short Inter XH3 .. XHn     H21M     ..H21M     .       1.96 Ang.
                                          2-x,1-y,2-z  =      2_767 Check
```

Author Response: The unresolved thermal disorder can affect the H...H distances.

```
PLAT934_ALERT_3_B Number of (Iobs-Icalc)/Sigma(W) > 10 Outliers ..          6 Check
                8 -1  2,   4 -6  3,  -7 -4  5,   0  4  6,  -6 -7 10,  -6 -8 11,
```

Author Response: This is a result of limited data quality.

Compound **7**

```
PLAT084_ALERT_3_B High wR2 Value (i.e. > 0.25) ...................       0.43 Report
PLAT971_ALERT_2_B Check Calcd Resid. Dens.  1.53Ang From C04B           3.37 eA-3
```

Author Response: These results are a consequence of large amounts of disorders in the crystal.

Compound **8**

```
PLAT084_ALERT_3_B High wR2 Value (i.e. > 0.25) ...................       0.42 Report
PLAT220_ALERT_2_B NonSolvent   Resd 2  C   Ueq(max)/Ueq(min) Range         8.2 Ratio
```

Author Response: These results are a consequence of large amounts of disorders in the crystal.

3-2. Electronic Absorption Spectra

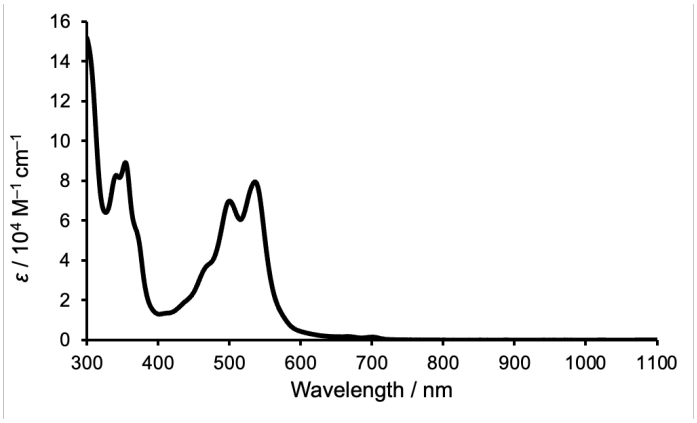

Supplementary Fig. 20. Electronic absorption spectrum of **1** in $CHCl_3$.

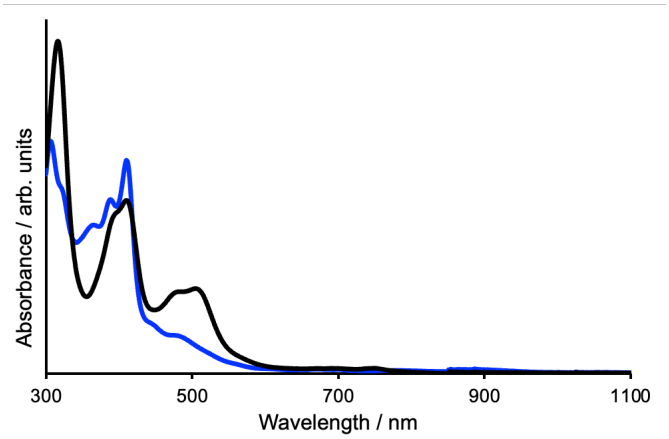

Supplementary Fig. 21. Electronic absorption spectra of **2** in CH_2Cl_2 before (blue) and after (black) addition of CF_3COOH (excess).

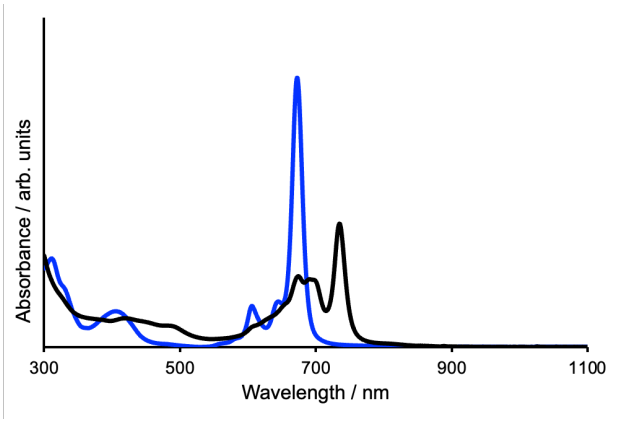

Supplementary Fig. 22. Electronic absorption spectra of **S1** in CH_2Cl_2 before (blue) and after (black) addition of CF_3COOH (excess).

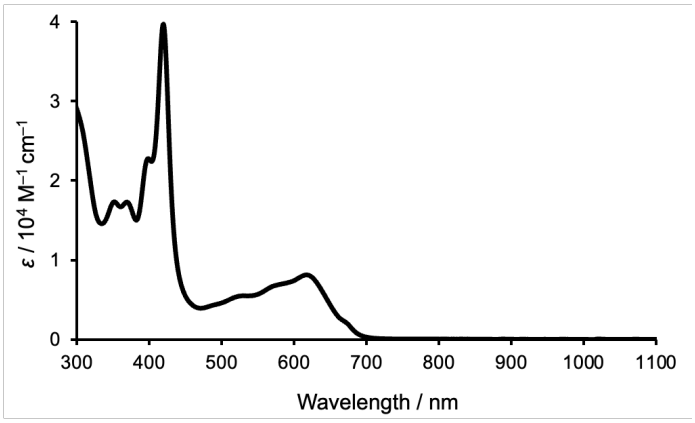

Supplementary Fig. 23. Electronic absorption spectrum of **7** in $CHCl_3$.

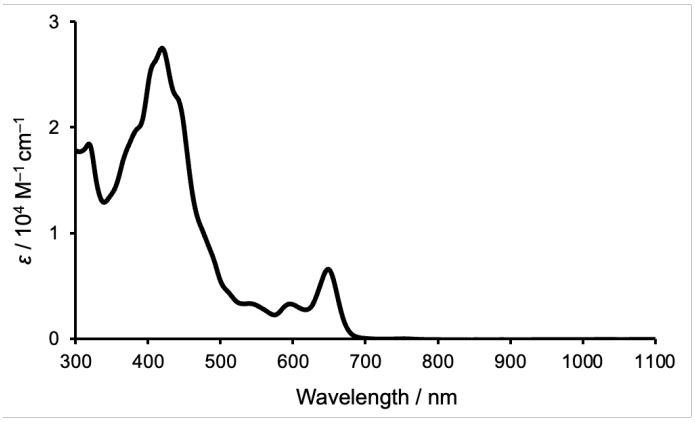

Supplementary Fig. 24. Electronic absorption spectrum of **8** in $CHCl_3$.

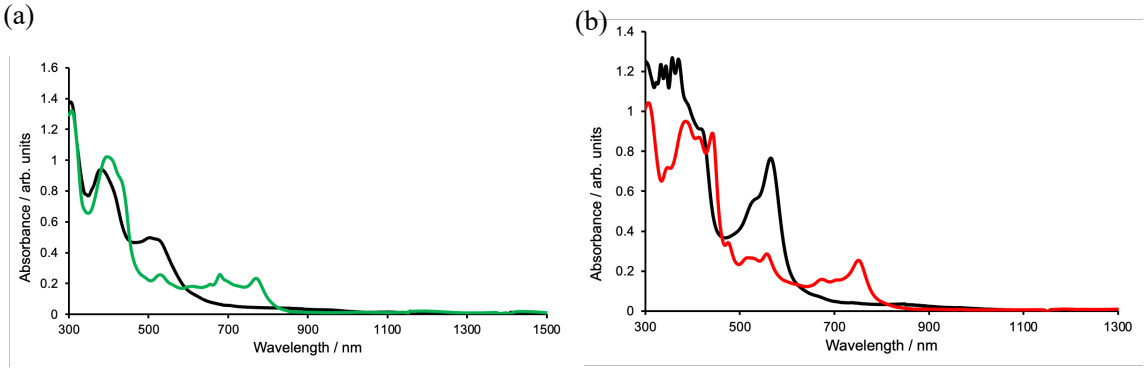

Supplementary Fig. 25. (a) Electronic absorption spectra of **3** in $CHCl_3$ before (green) and after (black) addition of $NOBF_4$ (excess). (b) Electronic absorption spectra of **4** in $CHCl_3$ before (red) and after (black) addition of $NOBF_4$ (excess).

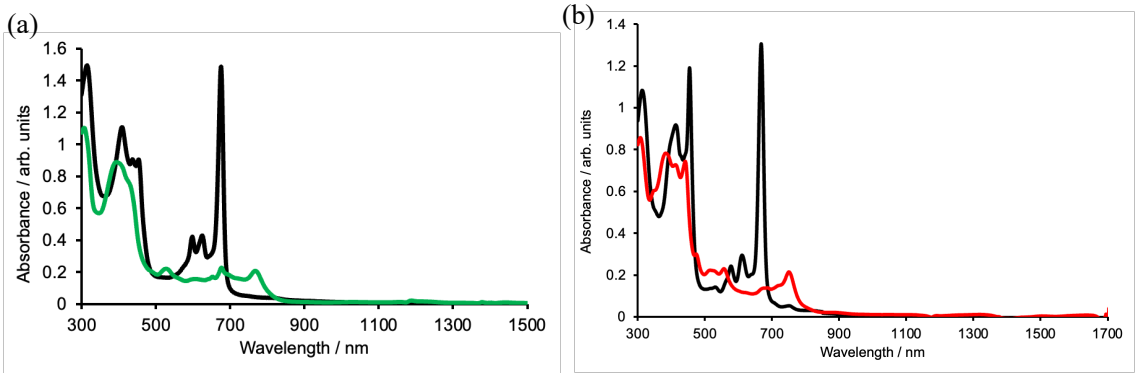

Supplementary Fig. 26. (a) Electronic absorption spectra of **3** in THF before (green) and after (black) addition of $CoCp_2$ (1.3 eq.). (b) Electronic absorption spectra of **4** in THF before (red) and after (black) addition of $CoCp_2$ (2.2 eq.).

3-3. Cyclic Voltammetry Measurements

The voltammograms were measured with a Hokuto Denko HZ-110 voltammetric analyzer at room temperature using a Ag/AgCl reference electrode, a platinum counter electrode, and a glassy carbon disk working electrode. The scan rate was 100 mV/s. Ferrocene was used as an internal standard for the reference of potential (V). The general procedure for the measurements is as follows: $^{n}Bu_4NBF_4$ (0.2 mmol) and CH_2Cl_2 (2 mL) were placed in a vial under an Ar atmosphere. To the solution was added the sample (0.002 mmol). Ar was bubbled into the solution for 5 min, and the voltammograms were recorded. Ferrocene was added to the solution as an internal standard at the end of the measurements.

Supplementary Table 5. Summary of redox potentials of **2**, **3**, and **4** in CH_2Cl_2.

	2	**3**	**4**
$E_{red,1/2}$ (V vs Fc/Fc^+)	–1.11 –1.46	–0.73	–0.85
$E_{ox,1/2}$ (V vs Fc/Fc^+)		–0.17	–0.28
$E_{ox,pa}$ (V vs Fc/Fc^+)	+0.43		
$E_{red,pa}$ (V vs Fc/Fc^+)	–1.06		

4. Computational Details

All calculations were performed at the Density Functional Theory (DFT), by means of (U)M06[6] functional as implemented in Gaussian 16.[7] We used the 6-31G(d,p) basis set for H, C, and N and the LANL2DZ basis set for Ni. NBO spin calculations were performed with NBO 3.1 package.[8] We computed compounds **2'** (M06), **3'**, and **4'** (UM06) without peripheral aryloxy groups as model compounds of **2**, **3**, and **4**, respectively (**Supplementary Fig. 27**). All the compounds were optimized as planar structures, except for the Ph group of **4'**, which is perpendicular to the tetrabenzodiazacorrole plane.

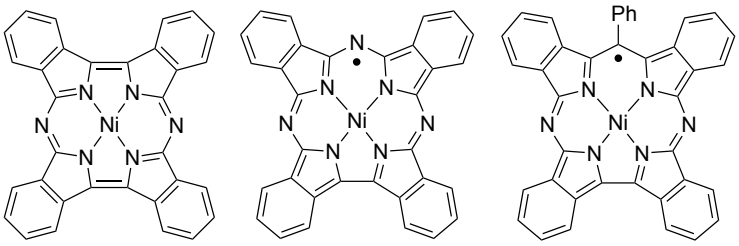

Supplementary Fig. 27. Structures of compounds **2'**, **3'**, and **4'** for computation.

Supplementary Table 6. Difference of total energies (kcal/mol) of singlet and triplet states of **2'**.

	Closed-shell singlet (RM06)	Open-shell singlet (UM06)	Open-shell triplet (UM06)
ΔE	0	not determined	+19.6

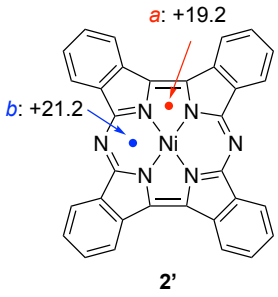

Supplementary Fig. 28. NICS(1) values (ppm) of **2'** computed at 1 Å above the center of each ring.

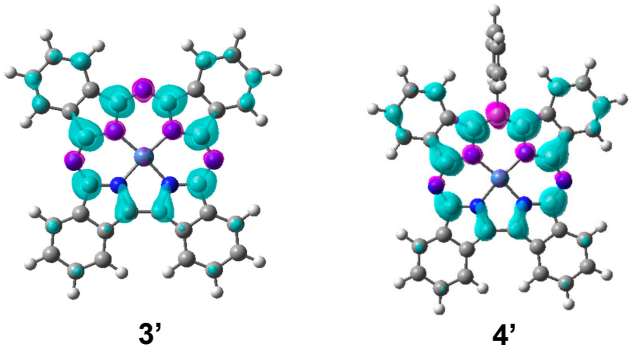

Supplementary Fig. 29. Calculated spin density distribution of **3'** and **4'**. MO = 0.02, Density = 0.0015.

Supplementary Table 7. TD-DFT calculation of **2'**.

	Energy [eV]	Energy [nm]	Oscillator Strength	Occupied MO		Unoccupied MO	Coefficient [%][a]
$S_0 \rightarrow S_1$	1.13	1096.38	0.0000	HOMO	→	LUMO	99.2
$S_0 \rightarrow S_2$	1.88	658.41	0.0368	HOMO–1	→	LUMO	98.4
$S_0 \rightarrow S_3$	2.21	561.09	0.0199	HOMO–2	→	LUMO	66.7
				HOMO–3	→	LUMO	28.6
$S_0 \rightarrow S_4$	2.53	490.81	0.0000	HOMO–4	→	LUMO	99.5
$S_0 \rightarrow S_5$	2.69	460.91	0.0664	HOMO–3	→	LUMO	59.7
				HOMO	→	LUMO+1	23.5
				HOMO–2	→	LUMO	15.8

[a] The coefficients greater than 10 % in the CI expansion are included.

Supplementary Table 8. TD-DFT calculation of **3'**.

	Energy [eV]	Energy [nm]	Oscillator Strength	Occupied MO		Unoccupied MO	Coefficient [%][a]
$D_0 \rightarrow D_1$	1.18	1054.19	0.0264	β-SOMO	→	β-SUMO	93.0
$D_0 \rightarrow D_2$	1.33	933.05	0.0000	β-SOMO–5	→	β-SUMO+3	49.0
$D_0 \rightarrow D_3$	1.62	764.29	0.0000	α-SOMO–2	→	α-SUMO+2	27.7
				β-SOMO–1	→	β-SUMO+3	25.8
				α-SOMO–13	→	α-SUMO+2	14.2
				β-SOMO–13	→	β-SUMO+3	11.7
$D_0 \rightarrow D_4$	1.77	702.45	0.0790	α-SOMO	→	α-SUMO	75.5
				β-SOMO–1	→	β-SUMO	19.8
$D_0 \rightarrow D_5$	1.83	677.80	0.0000	β-SOMO–2	→	β-SUMO+3	28.1
				α-SOMO–3	→	α-SUMO+2	26.3
				α-SOMO–14	→	α-SUMO+2	18.3
				β-SOMO–13	→	β-SUMO+3	16.6

[a] The coefficients greater than 10 % in the CI expansion are included.

Supplementary Table 9. TD-DFT calculation of **4'**.

	Energy [eV]	Energy [nm]	Oscillator Strength	Occupied MO		Unoccupied MO	Coefficient [%][a]
$D_0 \rightarrow D_1$	1.18	1186.95	0.0121	β-SOMO	→	β-SUMO	95.0
$D_0 \rightarrow D_2$	1.33	1095.62	0.0000	β-SOMO–6	→	β-SUMO+3	50.4
				α-SOMO–6	→	α-SUMO+2	50.3
$D_0 \rightarrow D_3$	1.62	853.62	0.0000	β-SOMO–1	→	β-SUMO+3	25.7
				α-SOMO–2	→	α-SUMO+2	20.9
				α-SOMO–16	→	α-SUMO+2	12.9
				β-SOMO–14	→	β-SUMO+3	10.2
$D_0 \rightarrow D_4$	1.77	745.15	0.0000	β-SOMO–2	→	β-SUMO+3	22.5
				β-SOMO–1	→	α-SUMO+2	17.6
				α-SOMO–15	→	α-SUMO+2	17.2
				β-SOMO–15	→	β-SUMO+3	13.7
				β-SOMO–16	→	β-SUMO+3	10.4
$D_0 \rightarrow D_5$	1.83	689.69	0.0660	α-SOMO	→	α-SUMO	69.4
				β-SOMO–1	→	β-SUMO	25.5

[a] The coefficients greater than 10 % in the CI expansion are included.

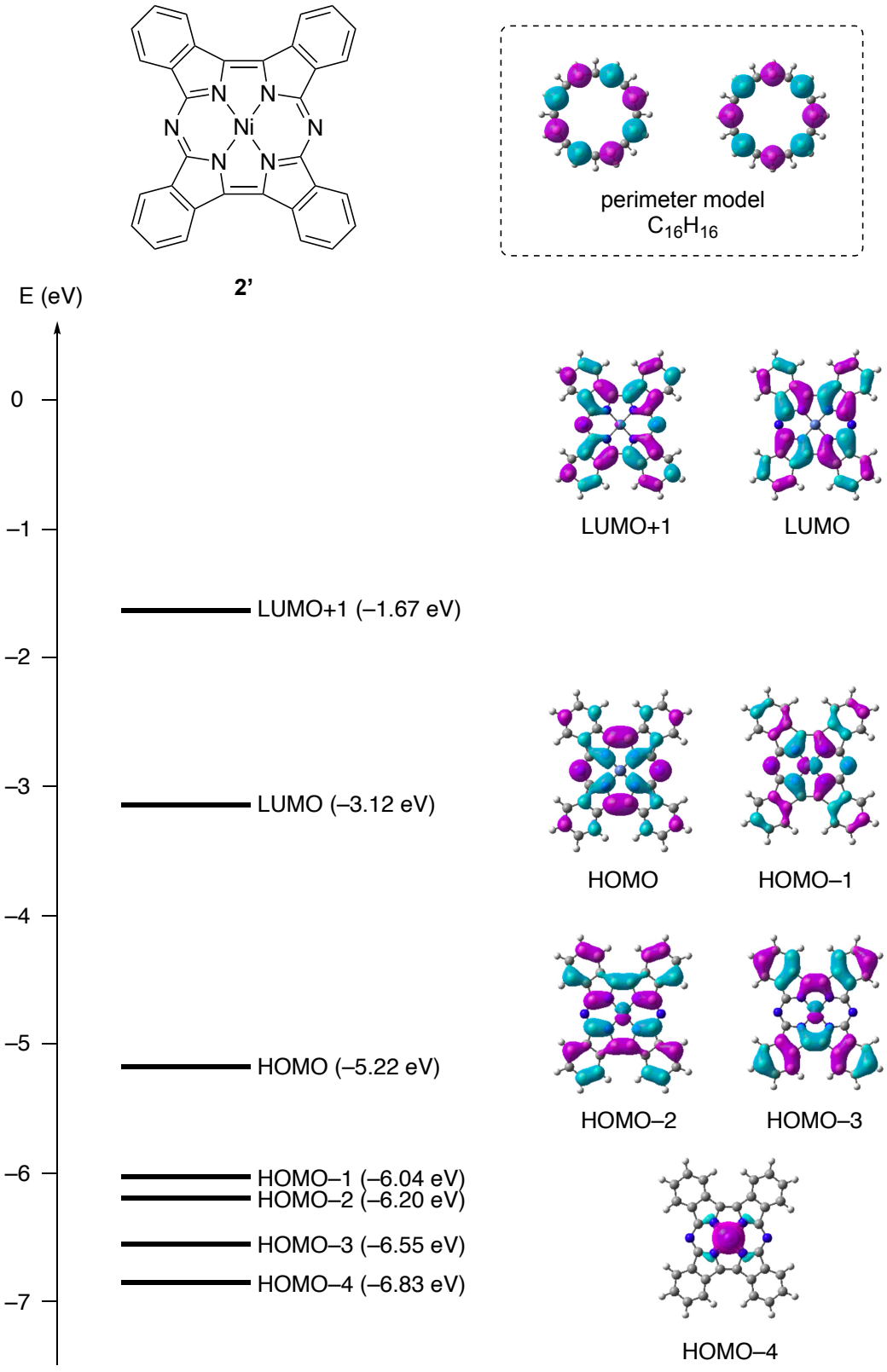

Supplementary Fig. 30. Frontier molecular orbitals of **2'**. Isovalue = 0.02.

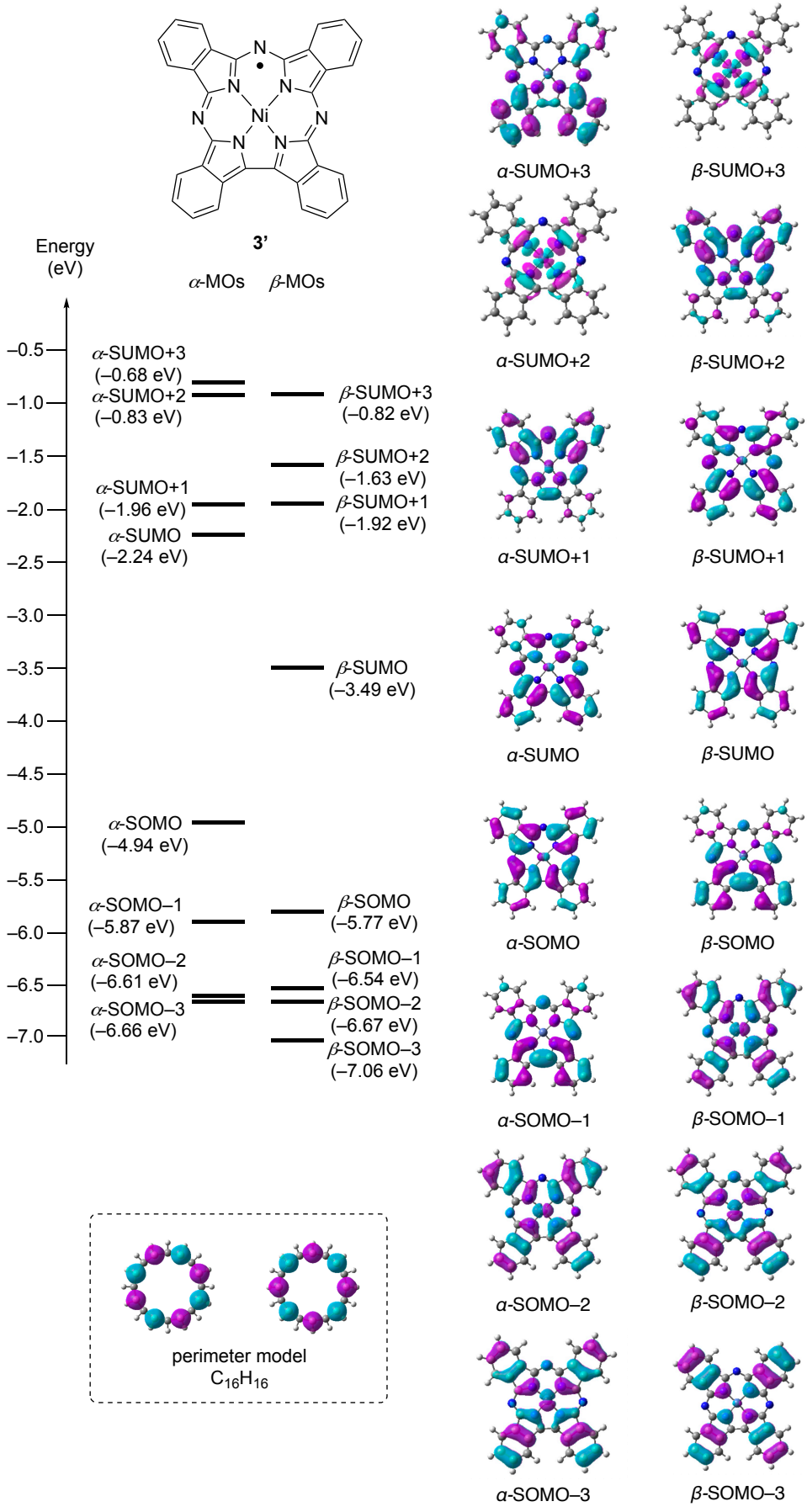

Supplementary Fig. 31. Frontier molecular orbitals of **3'**. Isovalue = 0.02.

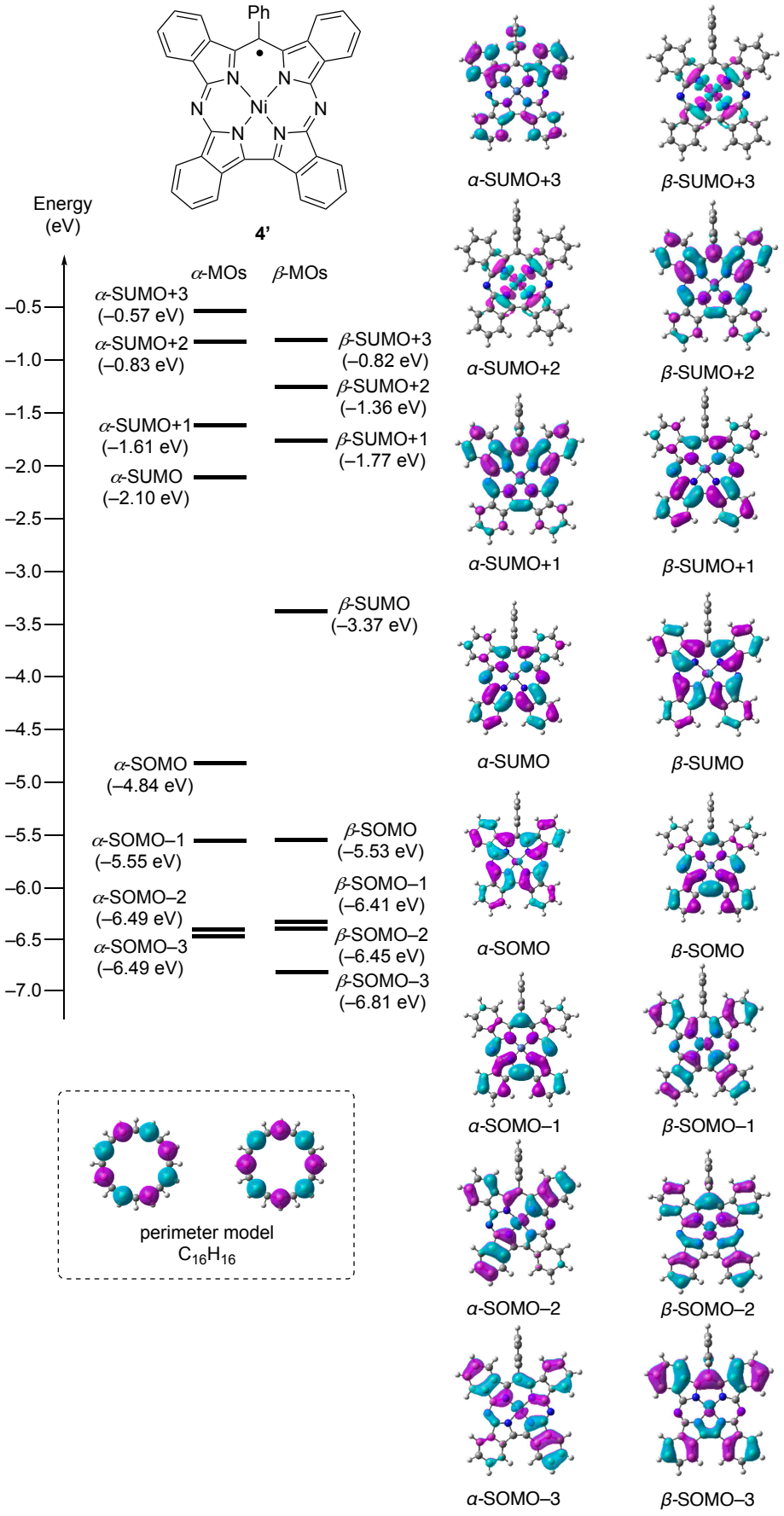

Supplementary Fig. 32. Frontier molecular orbitals of **4'**. Isovalue = 0.02.

5. NMR Spectra

^{1}H (500 MHz) in $CDCl_3$

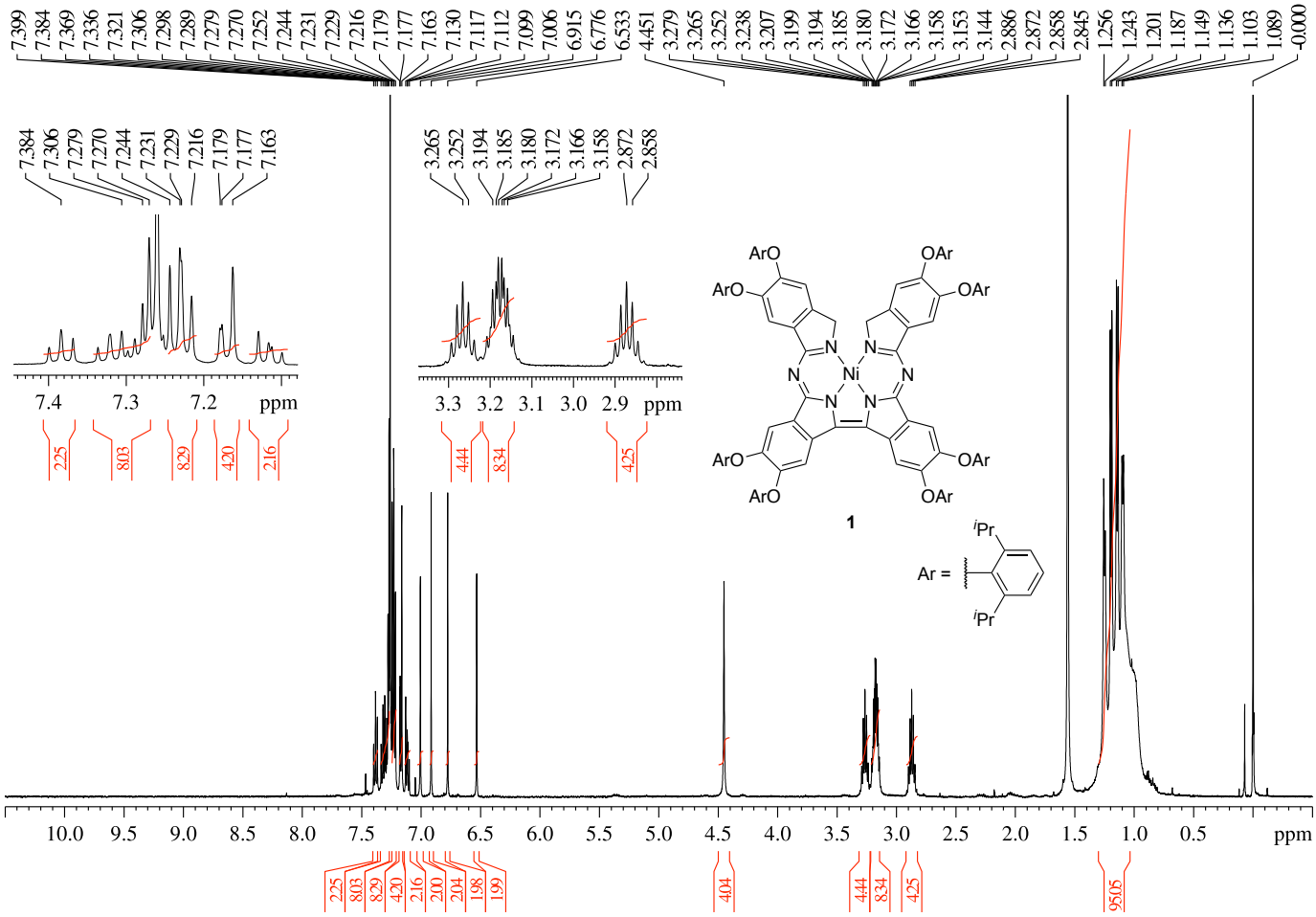

^{13}C (126 MHz) in $CDCl_3$

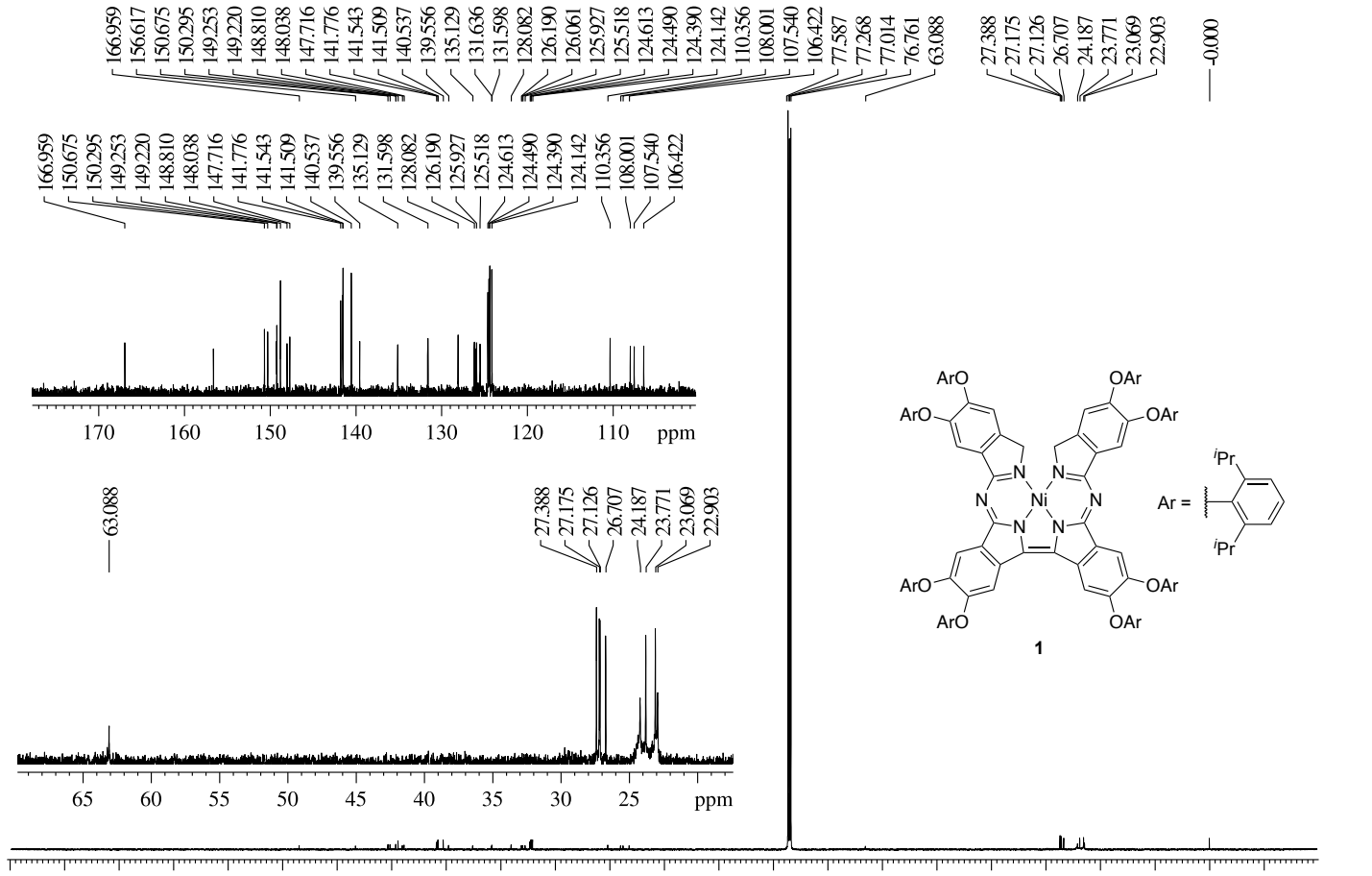

^{1}H (500 MHz) in $CDCl_3$

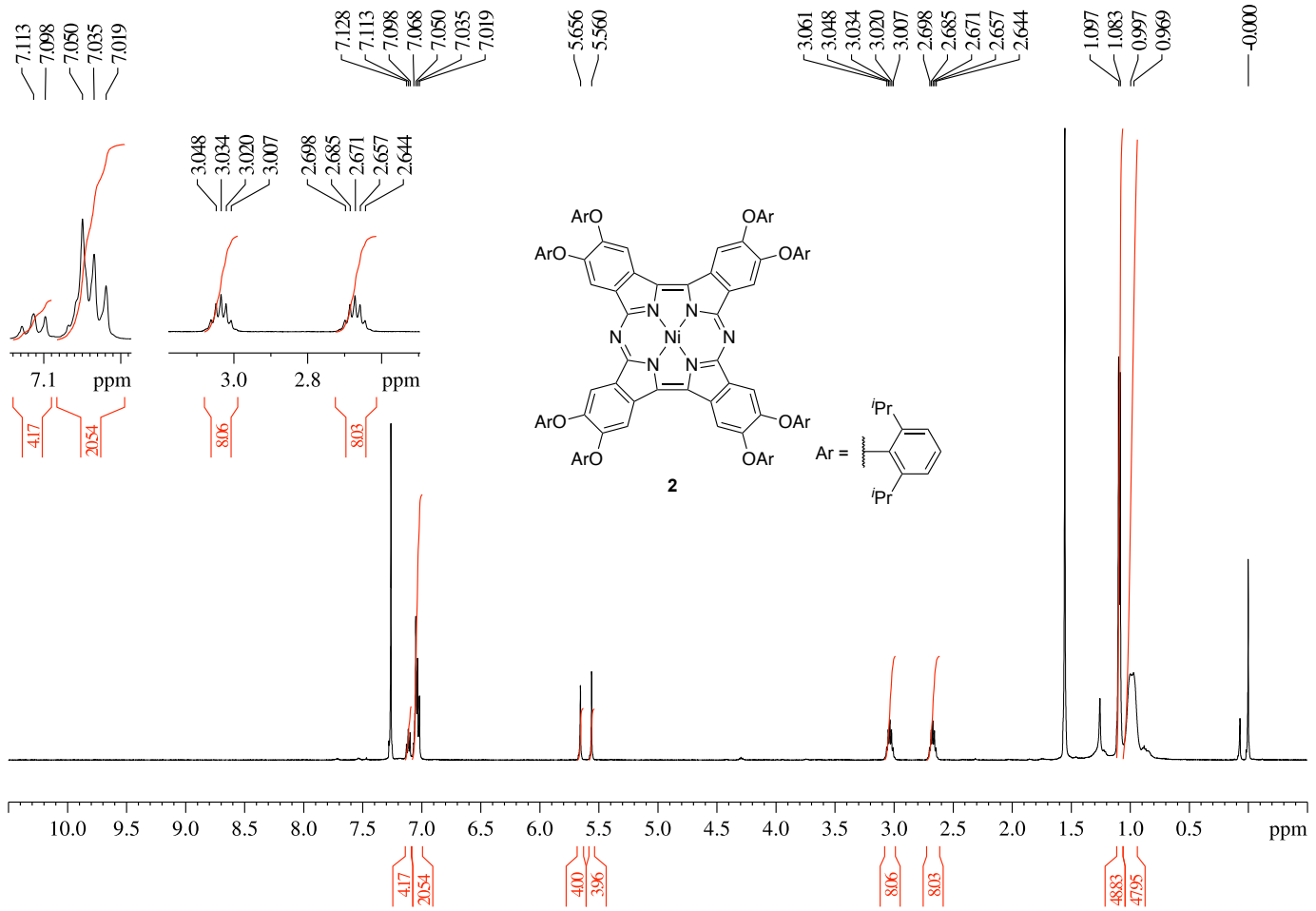

^{13}C (126 MHz) in $CDCl_3$

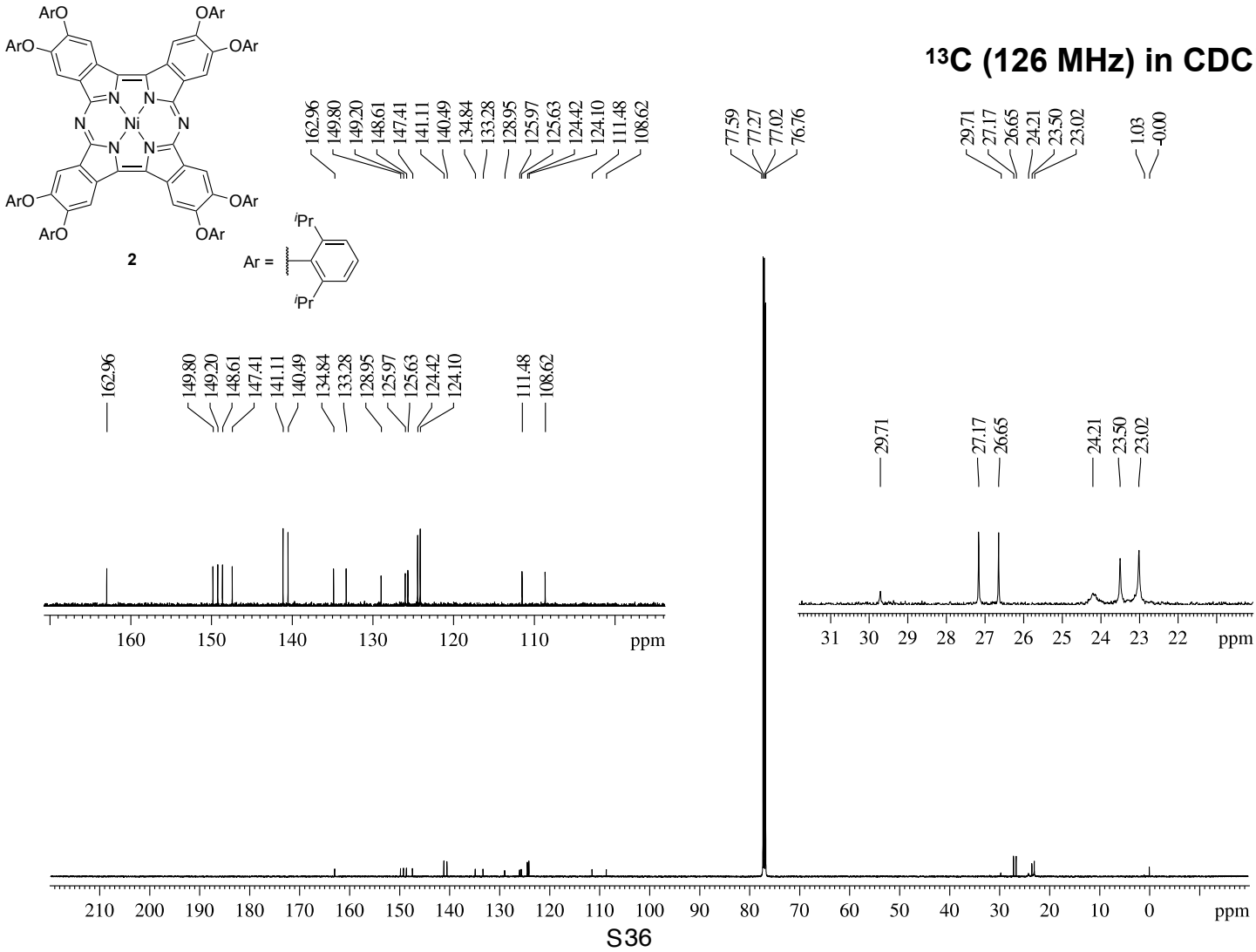

^{1}H (500 MHz) in pyridine-d_5

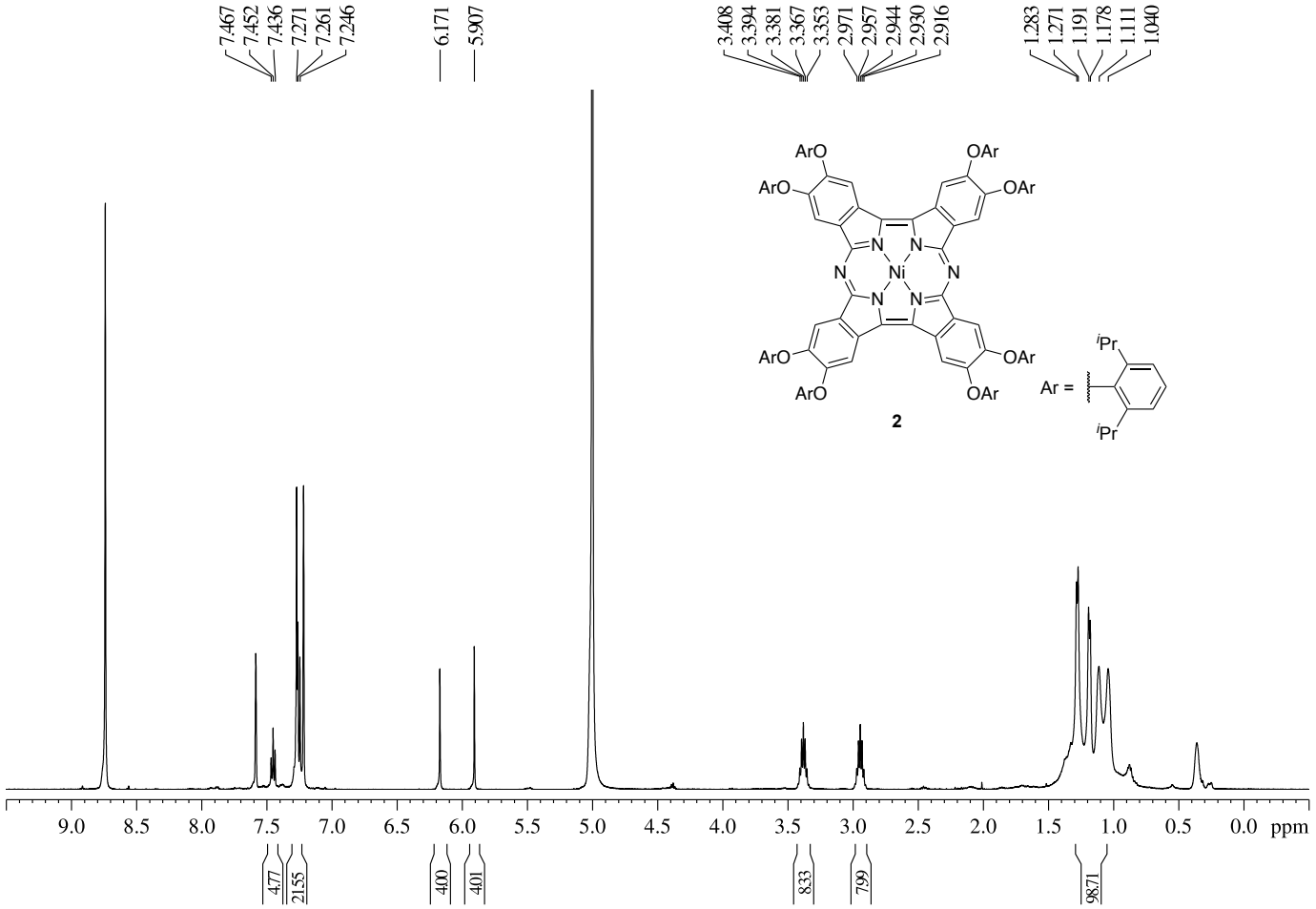

^{1}H (500 MHz) in $CDCl_3$

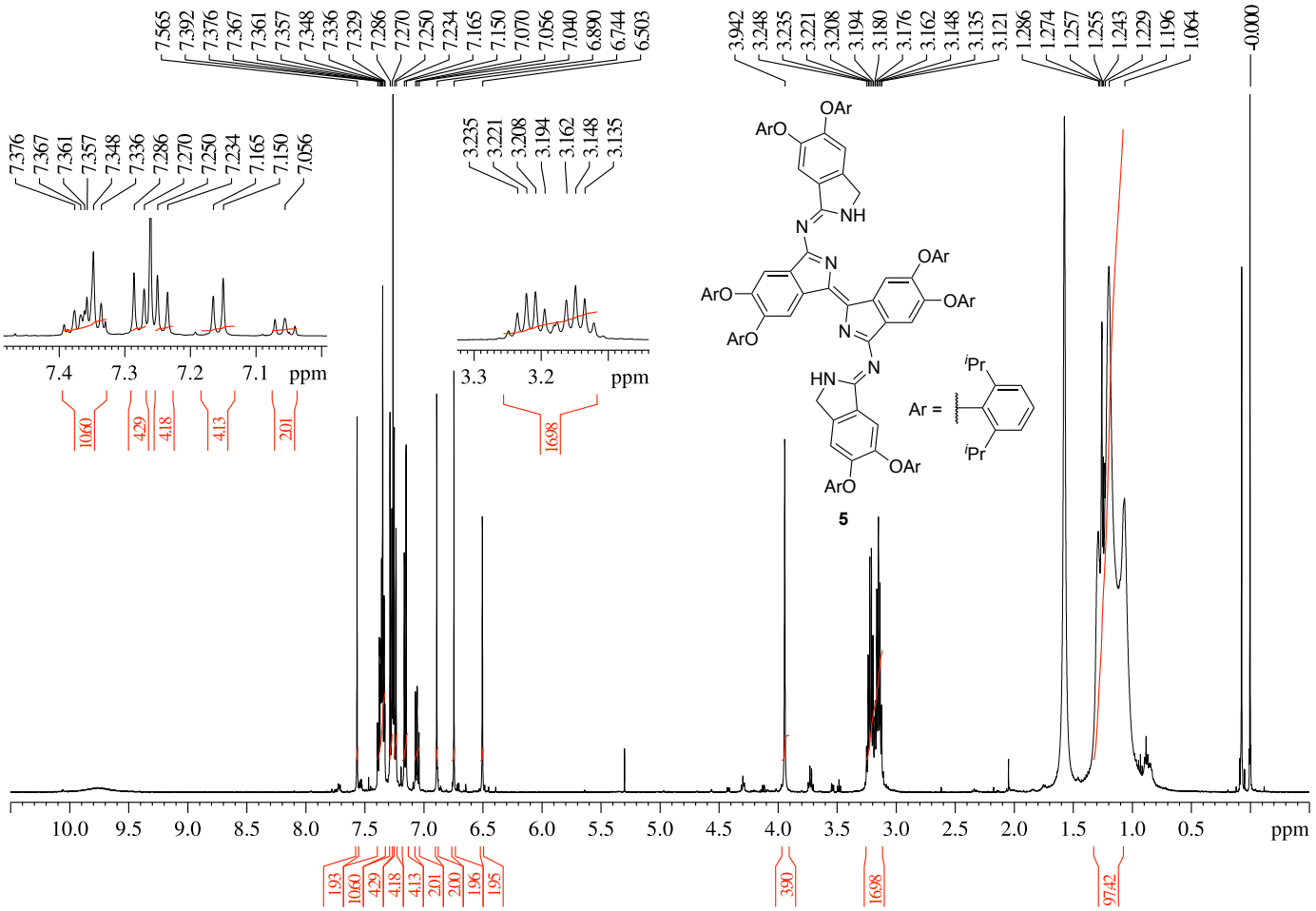

^{13}C (126 MHz) in $CDCl_3$

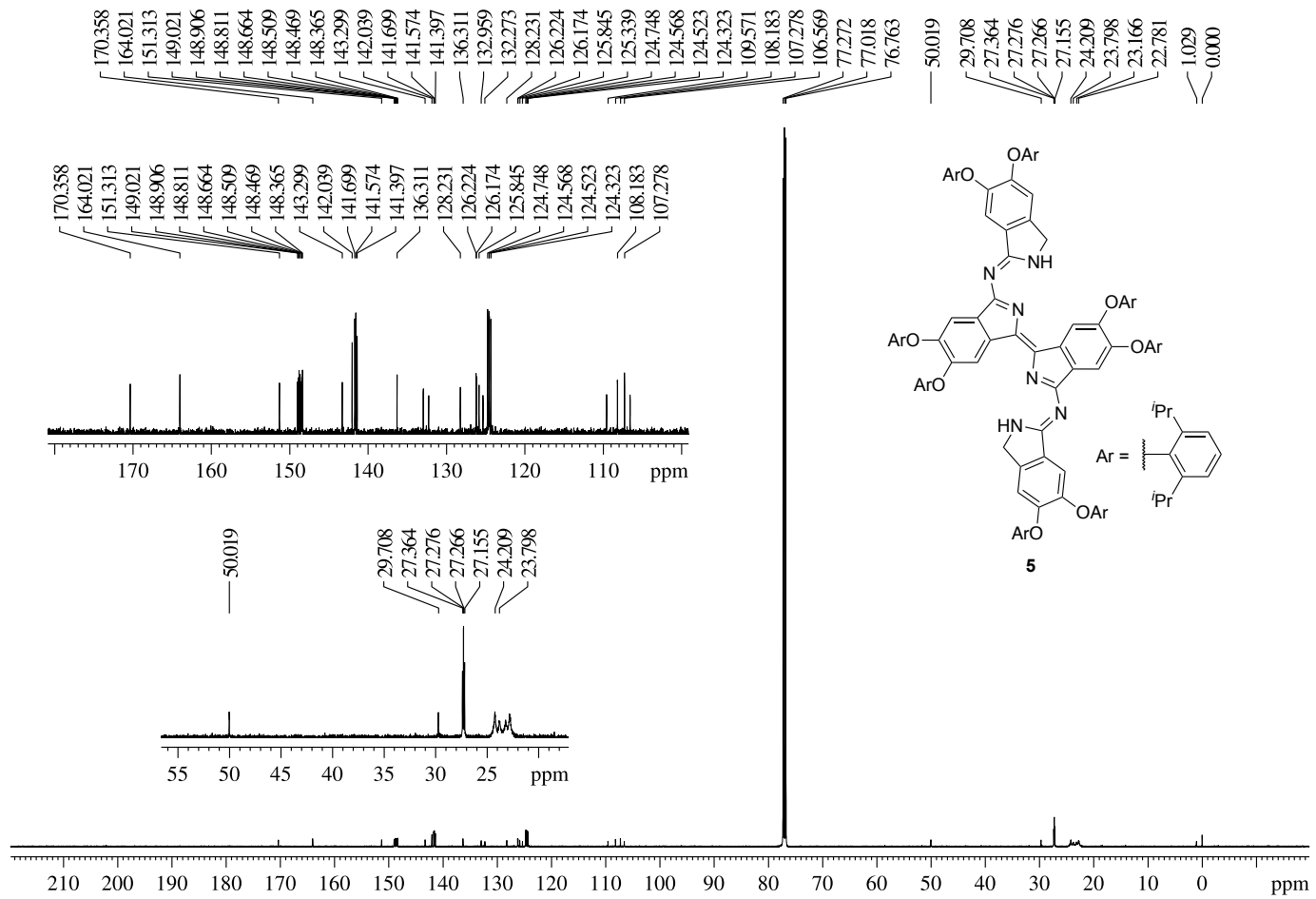

^{1}H (500 MHz) in $CDCl_3$

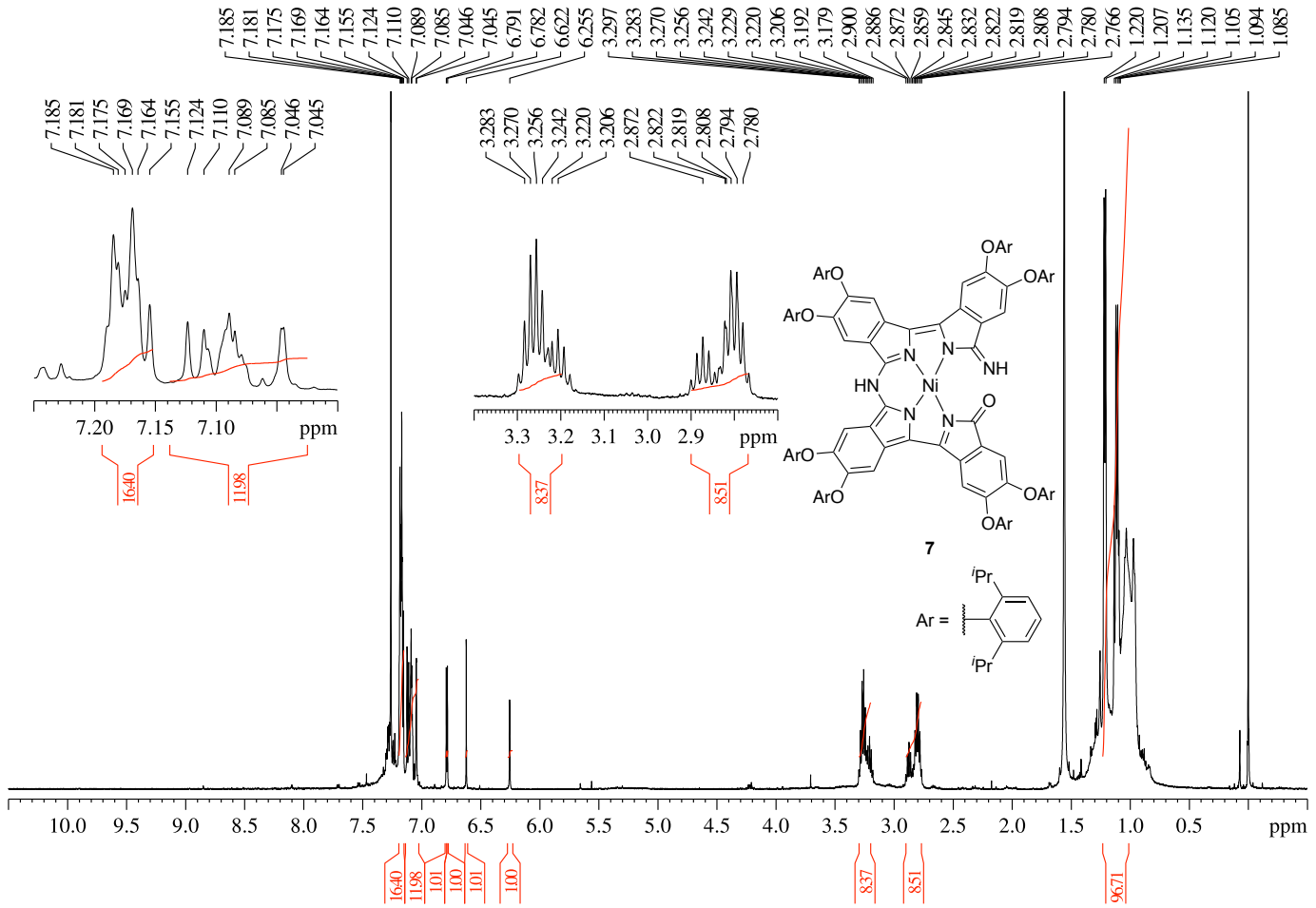

^{13}C (126 MHz) in $CDCl_3$

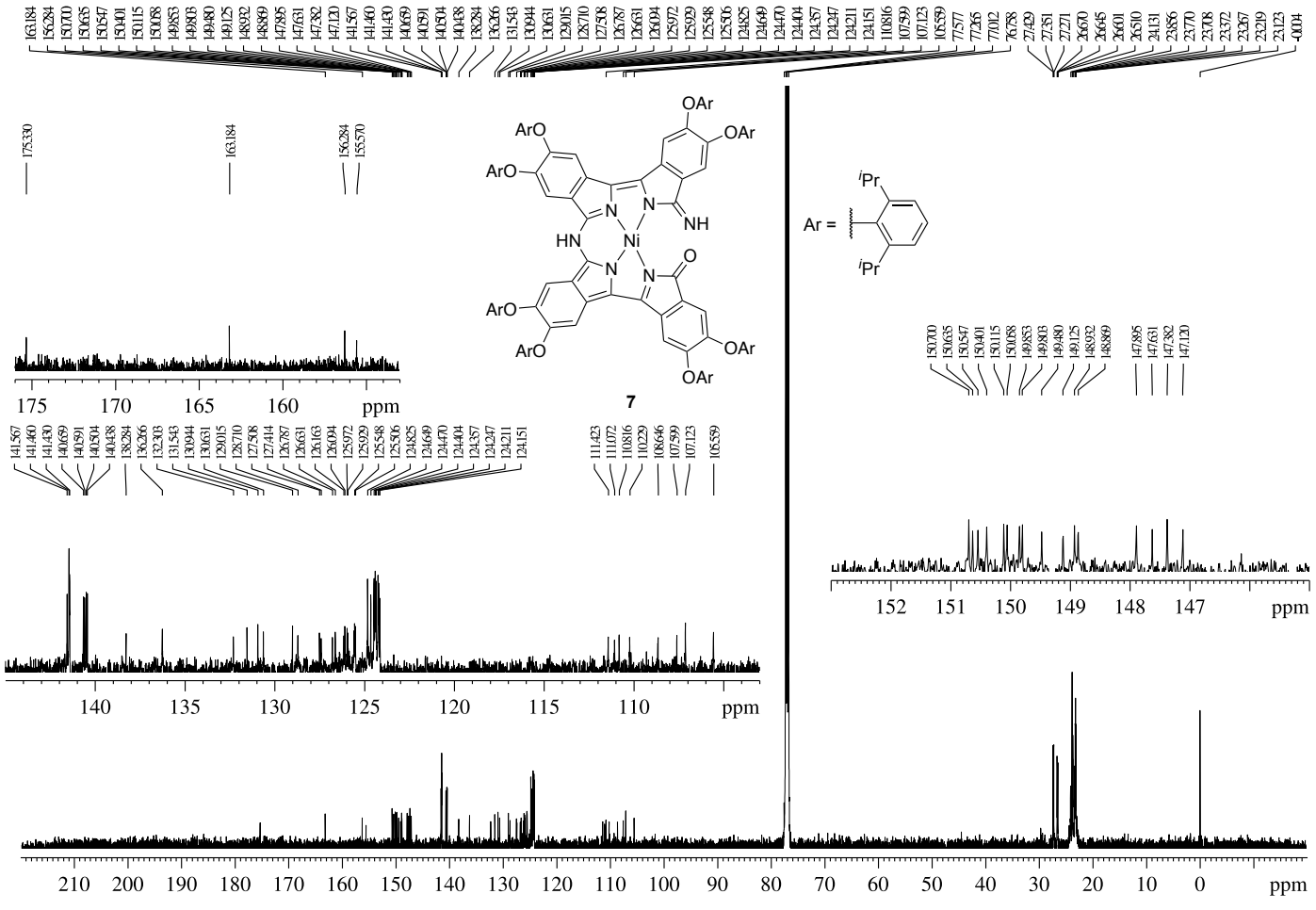

^{1}H (500 MHz) in CDCl$_3$/DMSO-d_6 (1:1)

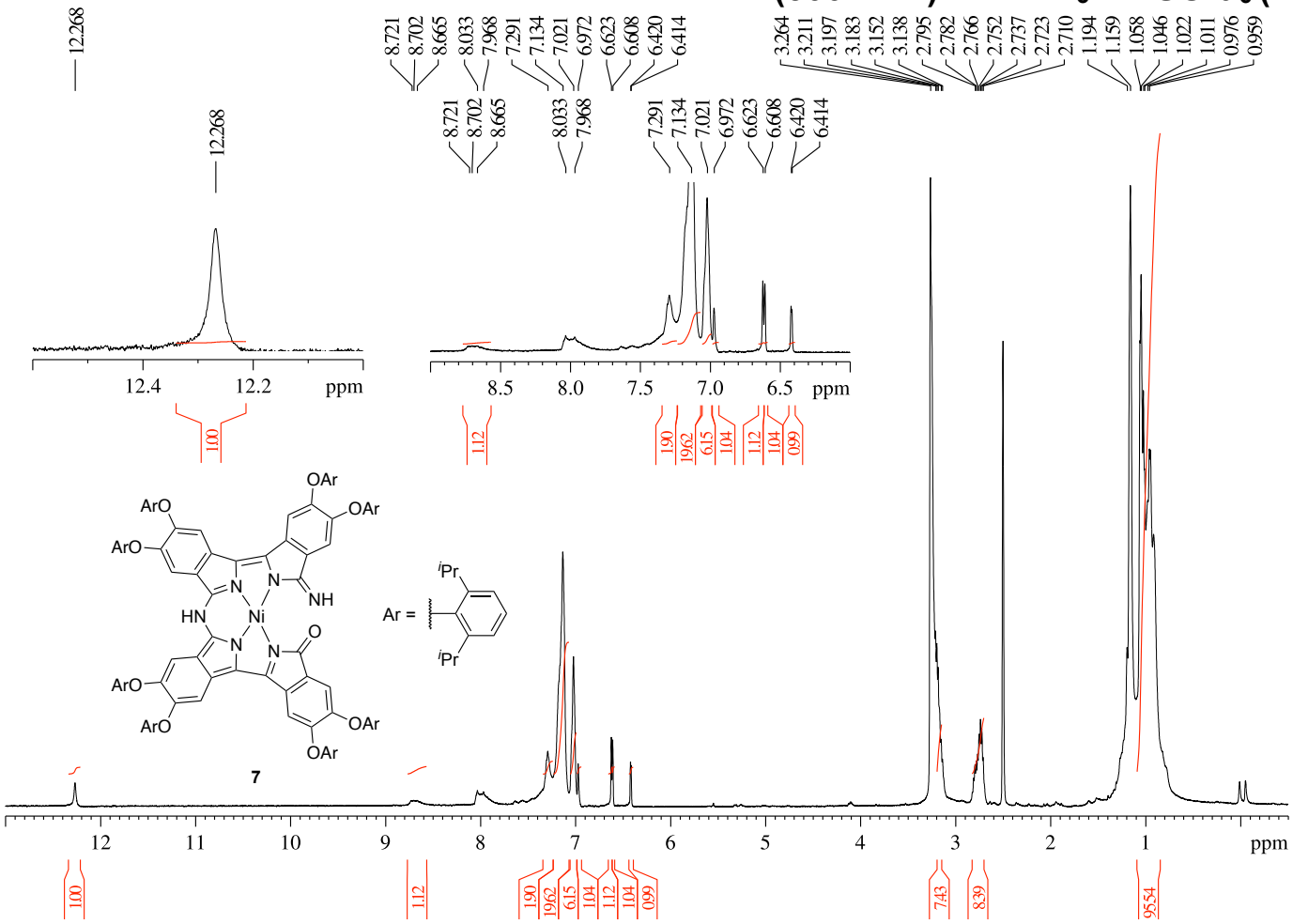

^{1}H (500 MHz) in CDCl$_3$/DMSO-d_6 (1:1) + D$_2$O

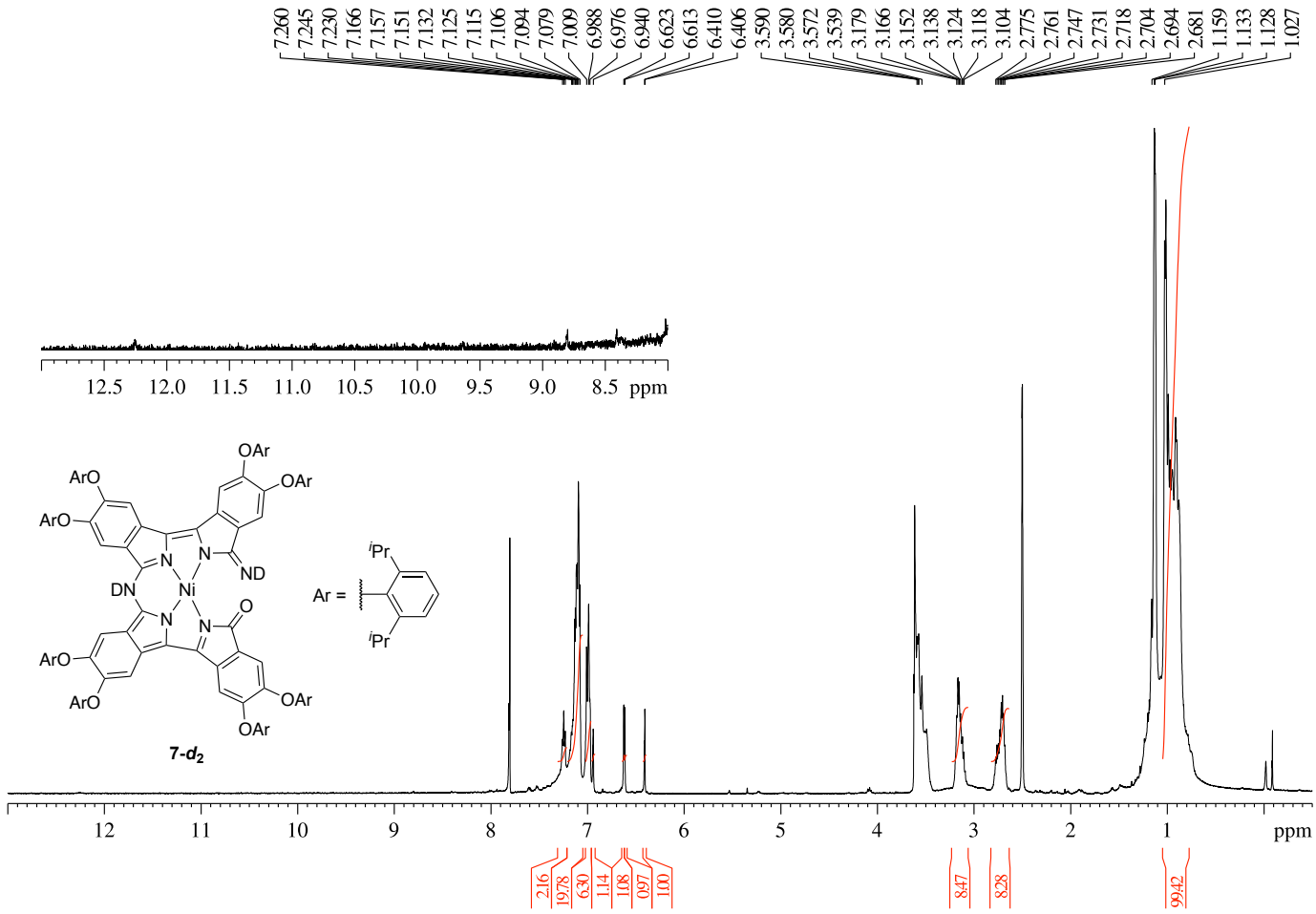

^{1}H (500 MHz) in $CDCl_3$

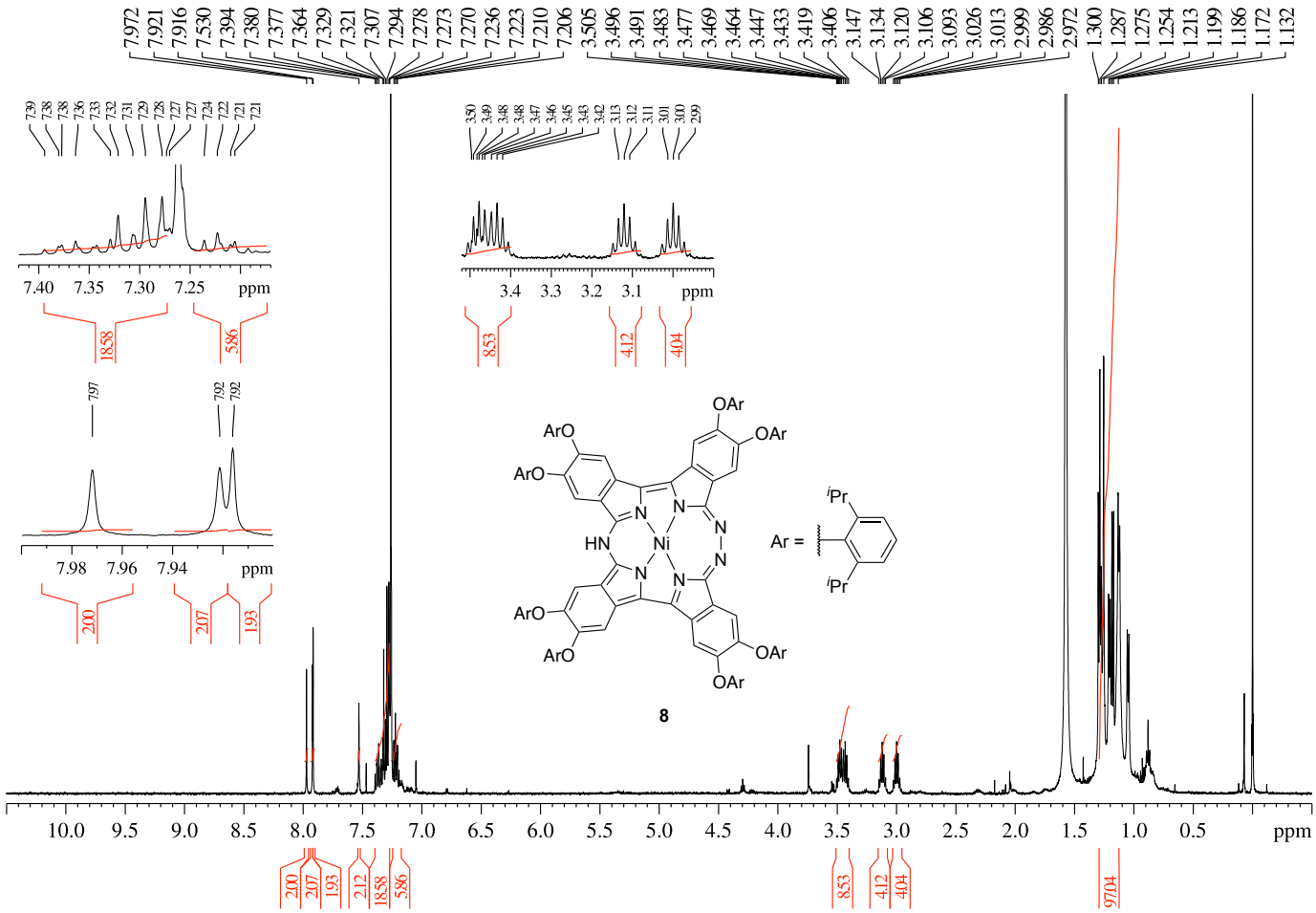

^{13}C (126 MHz) in $CDCl_3$

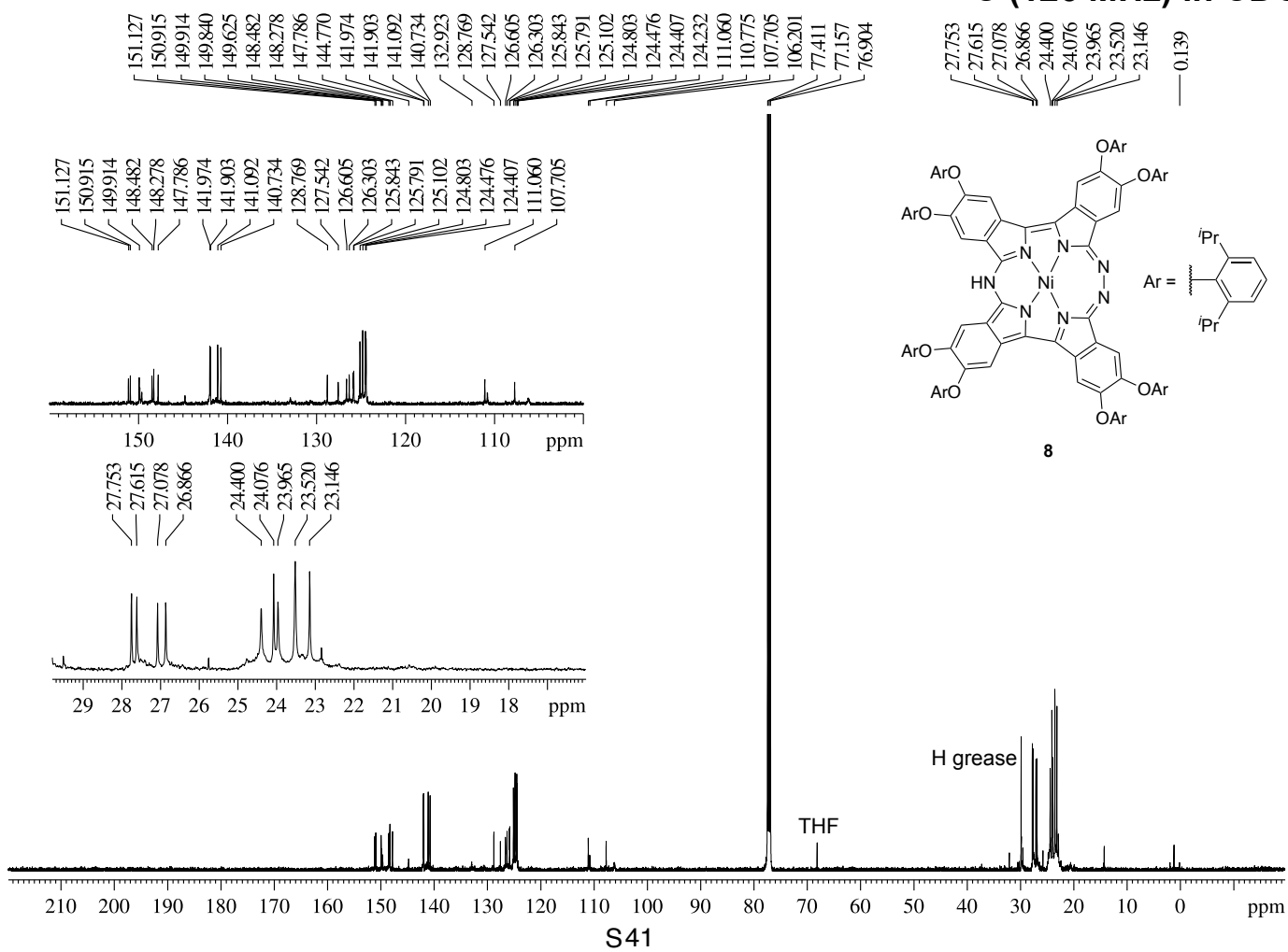

6. References

1. Tuhl, A.; Chidawanayika, W.; Ibrahim, H. M.; Al-Awadi, N.; Litwinski, C.; Nyokong, T.; Behbehani, H.; Manaa, H.; Makhseed, S. *J. Porphyrins Phthalocyanines* **2012**, *16*, 163.
2. Zhang, Y.; Wang, C.; Chen, X.; Pan, H.; Qi, D.; Wang, K.; Jiang, J. *Org. Chem. Front.* **2017**, *4*, 2364.
3. Sheldrick, G. M. *Acta Crystallogr., Sect. A* **2015**, *71*, 3.
4. Sheldrick, G. M. *Acta Crystallogr., Sect. C* **2015**, *71*, 3.
5. Dolomanov, O. V.; Bourhis, L. J.; Gildea, R. J.; Howard, J. A. K.; Puschmann, H. *J. Appl. Crystallogr*. **2009**, *42*, 339.
6. Zhao, Y.; Truhlar, D. G. *Theor. Chem. Acc.* **2008**, *120*, 215.
7. Gaussian 16, Revision B.01, Frisch, M. J.; Trucks, G. W.; Schlegel, H. B.; Scuseria, G. E.; Robb, M. A.; Cheeseman, J. R.; Scalmani, G.; Barone, V.; Petersson, G. A.; Nakatsuji, H.; Li, X.; Caricato, M.; Marenich, A. V.; Bloino, J.; Janesko, B. G.; Gomperts, R.; Mennucci, B.; Hratchian, H. P.; Ortiz, J. V.; Izmaylov, A. F.; Sonnenberg, J. L.; Williams-Young, D.; Ding, F.; Lipparini, F.; Egidi, F.; Goings, J.; Peng, B.; Petrone, A.; Henderson, T.; Ranasinghe, D.; Zakrzewski, V. G.; Gao, J.; Rega, N.; Zheng, G.; Liang, W.; Hada, M.; Ehara, M.; Toyota, K.; Fukuda, R.; Hasegawa, J.; Ishida, M.; Nakajima, T.; Honda, Y.; Kitao, O.; Nakai, H.; Vreven, T.; Throssell, K.; Montgomery, J. A., Jr.; Peralta, J. E.; Ogliaro, F.; Bearpark, M. J.; Heyd, J. J.; Brothers, E. N.; Kudin, K. N.; Staroverov, V. N.; Keith, T. A.; Kobayashi, R.; Normand, J.; Raghavachari, K.; Rendell, A. P.; Burant, J. C.; Iyengar, S. S.; Tomasi, J.; Cossi, M.; Millam, J. M.; Klene, M.; Adamo, C.; Cammi, R.; Ochterski, J. W.; Martin, R. L.; Morokuma, K.; Farkas, O.; Foresman, J. B.; Fox, D. J. Gaussian, Inc., Wallingford CT, **2016**.
8. Glendening, E. D.; Reed, A. E.; Carpenter, J. E.; Weinhold, F. NBO Version 3.1; **1990**.